2015

Lifetime of the electroweak vacuum and sensitivity to Planck scale physics

Vincenzo Branchina

Emanuele Messina

Marc Sher
College of William and Mary

Recommended Citation

Branchina, V., Messina, E., & Sher, M. (2015). Lifetime of the electroweak vacuum and sensitivity to Planck scale physics. Physical Review D, 91(1), 013003.

PHYSICAL REVIEW D **91,** 013003 (2015)

Lifetime of the electroweak vacuum and sensitivity to Planck scale physics

Vincenzo Branchina,[1,*] Emanuele Messina,[1,†] and Marc Sher[2,‡]
[1]*Department of Physics, University of Catania and INFN, Sezione di Catania, Via Santa Sofia 64, I-95123 Catania, Italy*
[2]*High Energy Theory Group, Department of Physics, College of William and Mary, Williamsburg, Virginia 23187-8795, USA*
(Received 28 August 2014; published 14 January 2015)

If the Standard Model (SM) is valid up to extremely high energy scales, then the Higgs potential becomes unstable at approximately 10^{11} GeV. However, calculations of the lifetime of the SM vacuum have shown that it vastly exceeds the age of the Universe. It was pointed out by two of us (V. B., E. M.) that these calculations are extremely sensitive to effects from Planck scale higher-dimensional operators and, without knowledge of these operators, firm conclusions about the lifetime of the SM vacuum cannot be drawn. The previous paper used analytical approximations to the potential and, except for Higgs contributions, ignored loop corrections to the bounce action. In this work, we do not rely on any analytical approximations and consider all contributions to the bounce action, confirming the earlier result. It is surprising that the Planck scale operators can have such a large effect when the instability is at 10^{11} GeV. There are two reasons for the size of this effect. In typical tunneling calculations, the value of the field at the center of the critical bubble is much larger than the point of the instability; in the SM case, this turns out to be numerically within an order of magnitude of the Planck scale. In addition, tunneling is an inherently nonperturbative phenomenon and may not be as strongly suppressed by inverse powers of the Planck scale. We include effective Φ^6 and Φ^8 Planck-scale operators and show that they can have an enormous effect on the tunneling rate.

DOI: 10.1103/PhysRevD.91.013003 PACS numbers: 14.80.Bn, 11.10.Hi, 11.27.+d, 12.15.-y

I. INTRODUCTION

Shortly after the Standard Model (SM) was established, it was pointed out in a seminal paper by Cabibbo *et al.* [1] that the quartic scalar coupling could either become nonperturbative or become negative before the unification scale is reached. In the former case, new physics would have to intervene, and in the latter case the potential would become metastable; requiring that neither of these occur led to bounds on the Higgs and fermion masses. Over the decades, this calculation has been increasingly refined [2–18].

While several different scenarios for physics beyond the Standard Model are possible, the conservative choice is to assume that the Standard Model is valid all the way up to the Planck scale M_P, i.e. that new physics interactions only occur at M_P. This has been most recently investigated in Refs. [19–23]. According to these analyses, the recently measured value of the Higgs boson mass [24,25] is, in conjunction with improved measurements of the top quark mass, tantalizingly close to the stability/metastability boundary. These calculations, however, show that the instability does occur at scales below the Planck scale.

The instability is primarily due to the top quark mass. Because of the loop corrections coming from the top, the Higgs effective potential $V_{\rm eff}(\phi)$ turns over for values of ϕ much larger than v, the location of the electroweak (EW) minimum, and develops a new minimum at $\phi_{\rm min} \gg v$. Depending on SM parameters, in particular on the top and Higgs masses, M_t and M_H, the second minimum can be higher or lower than the EW one. In the first case, the EW vacuum is stable, and in the second one it is metastable and we have to consider its lifetime τ. Normalizing $V_{\rm eff}(\phi)$ so that it vanishes at $\phi = v$, in the case when $V_{\rm eff}(\phi_{\rm min}) < V_{\rm eff}(v)$, the instability scale $\phi_{\rm inst}$ is the value of ϕ such that $V_{\rm eff}(\phi_{\rm inst}) = 0$: for $\phi > \phi_{\rm inst}$, the potential becomes negative, later developing the new minimum. For the Higgs and top masses given by the current central experimental values, $M_H \sim 125.7$ GeV and $M_t \sim 173.34$ GeV, $\phi_{\rm inst} \sim 10^{11}$ GeV $\gg v$.

The results are usually summarized with the help of the stability phase diagram of Fig. 1, where the (M_H, M_t) plane is divided into three different sectors: an absolute stability region, where $V_{\rm eff}(\phi_{\rm min}) > V_{\rm eff}(v)$; a (so-called) metastability region, where $V_{\rm eff}(\phi_{\rm min}) < V_{\rm eff}(v)$, but the lifetime, τ, is given by $\tau > T_U$; and an instability region, where $V_{\rm eff}(\phi_{\rm min}) < V_{\rm eff}(v)$ but $\tau < T_U$ (T_U is the age of the Universe). The stability (dashed) line separates the stability and the metastability sectors. The instability (dot-dashed) line separates the metastability and the instability regions and is obtained for M_H and M_t such that $\tau = T_U$.

This stability phase diagram is obtained by considering SM interactions only, as it is usually argued [18–22] that new physics interactions at the Planck scale, although present, have no impact on it. This argument seems quite reasonable,

*branchina@ct.infn.it
†emanuele.messina@ct.infn.it
‡mtsher@wm.edu

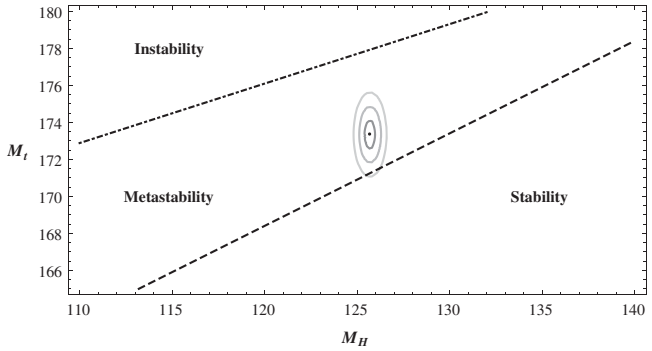

FIG. 1. The stability phase diagram according to the standard analysis, i.e. in the absence of new interactions at the Planck scale. The M_H-M_t plane is divided into three sectors: absolute stability, metastability, and instability regions. The dot indicates $M_H \sim 125.7$ GeV and $M_t \sim 173.34$ GeV. The ellipses take into account 1σ, 2σ, and 3σ, according to the current experimental errors.

since the instability occurs at scales of $\sim 10^{11}$ GeV and new physics interactions are suppressed by powers of the inverse Planck scale. If this is really the case, from Fig. 1, we learn that for the current experimental values of M_H and M_t, the electroweak vacuum is metastable, with a lifetime much larger than the age of the Universe [18,21,22], and also that we are very close to the stability line (so-called "criticality"), so that a better determination of M_H and M_t would allow us to discriminate among a metastable, a stable, or a critical vacuum state for our universe [26,27]. Some authors consider this "near criticality" of the SM as the most important message from the data on the Higgs boson [23]. We note that this is also needed for the Higgs inflation scenario of [28] (see also [29–31]).

For $M_H = 125.7$ GeV and $M_t \sim 173.34$ GeV, $\phi_{\rm inst} \sim 10^{11}$ GeV. For $\phi > \phi_{\rm inst}$, $V_{\rm eff}(\phi)$ is negative and decreasing. For $\phi \geq M_P$, the potential continues to decrease for a long while, forming a new minimum at a scale $\phi_{\rm min}$ much larger than M_P, $\phi_{\rm min} \sim 10^{30}$ GeV. Of course, one expects Planck scale operators to have an effect long before that scale is reached.

It is usually argued [18] that this potential must be eventually stabilized by the unknown new physics around M_P. In other words, these new physics interactions are expected to modify $V_{\rm eff}(\phi)$ around M_P in such a way as to lead to a new minimum around this scale. However, it is also argued that the computation of the lifetime τ of the electroweak vacuum can still be performed with the help of the unmodified Higgs potential $V_{\rm eff}(\phi)$, obtained with SM interactions only.[1]

[1]Some effects of TeV-scale higher-dimensional operators on vacuum stability were considered in an early paper [32], although tunneling rates were not. The possibility of the transition occurring during inflation was considered in [33]. For recent work on modifications induced by the coupling of the Higgs field to gravity or to dark matter candidates, see [34] and [35].

As the instability occurs for very large values of ϕ ($\phi_{\rm inst} \sim 10^{11}$ GeV), $V_{\rm eff}(\phi)$ is well approximated by keeping only the quartic term [11]. Therefore, following [36–38], the electroweak vacuum lifetime is computed by considering first the bounce solution to the Euclidean equation of motion for the classical potential $V(\phi) = \frac{\lambda}{4}\phi^4$ with a negative value of λ, and then taking into account the quantum fluctuations around the bounce.

It has recently been shown, however, that new physics at M_P can enormously modify the tunneling time and, more generally, the stability phase diagram [39–41]. For the purposes of illustrating this effect, the analysis in [39] was performed by considering two major simplifications. An approximation for the modified Higgs potential was considered that allowed for the existence of analytical bounce solutions; and only the quantum fluctuations coming from the Higgs sector were considered.

In the present paper, the analysis of [39] is improved, extended, and completed in the following important aspects. First of all, we do not consider any approximation for the potential. Therefore, as we can no longer rely on analytical tools, we look for numerical bounce solutions for the complete potential. Also, the quantum fluctuation corrections to τ are computed by considering the contributions from all of the different sectors of the theory. This more complete analysis, as we shall see, confirms the results presented in [39] and provides the theoretical support for the results presented in [41], where some of the results presented in this work were anticipated and used.

The rest of the paper is organized as follows. In the next section, we review the calculation of the electroweak vacuum lifetime in the Standard Model. It is shown there that the standard assumption that Planck scale operators can be neglected may not be valid, since the value of the field in the center of the critical bubble is much larger than the instability scale, and is close to the Planck scale. In Sec. III, the effects of Planck scale operators are then included. In Sec. IV, we compare the numerical results with the analytic results of Ref. [39], and Sec. V contains our conclusions. There are three appendixes. In Appendix A, the computation of the quantum fluctuation contribution to the tunneling time is presented in some detail. Appendix B provides some tools for the numerical computation of the bounce. In particular, the bounce considered in Sec. III is computed. In Appendix D, we provide an explicit example, using $SU(5)$, giving the size of the higher dimensional operators.

II. BOUNCES AND THE PLANCK SCALE M_P

Before starting our analysis on the impact of new physics, in the present section we focus our attention on the standard analysis, where it is assumed that the stability phase diagram and, in particular, the lifetime of the electroweak vacuum τ are not affected by new physics at the Planck scale [18–22].

Let us begin by considering the Euclidean action for the scalar sector of the SM

$$S[\Phi] = \int d^4x((\partial_\mu \Phi)^\dagger \cdot (\partial_\mu \Phi) + V(\Phi)), \tag{1}$$

where we write the scalar doublet Φ as

$$\Phi = \frac{1}{\sqrt{2}} \begin{pmatrix} -i(G_1 - iG_2) \\ \phi + iG_3 \end{pmatrix}, \tag{2}$$

with ϕ the Higgs field and G_i the Goldstone bosons, while the potential $V(\Phi)$ is, for large values of ϕ,

$$V(\Phi) = \lambda(\Phi^\dagger \Phi)^2. \tag{3}$$

The procedure for determining the tunneling rate was first discussed in Refs. [36–38], and a very clear discussion involving the Standard Model can be found in Ref. [42]. The bounce, ϕ_b, is a solution of the Euclidean equations of motion for the above action. Renaming for a moment S as the full SM action, following [42] we write for the tunneling probability (details are given in Appendix A)

$$p = \int \prod_{i=1}^{8} d\gamma_i J_{\text{zeros}}(\gamma_1, \ldots, \gamma_8) \left| \frac{\text{SDet}'(S''[\phi_b])}{\text{SDet}(S''[0])} \right|^{-1/2} e^{-S[\phi_b]}. \tag{4}$$

$S[\phi_b]$ is the tree-level action computed at $\phi = \phi_b$, with all of the other SM fields vanishing. S'' denotes double functional differentiation with respect to all of the SM fields. SDet is the superdeterminant, and Det′ means that in the computation of the determinant the zero modes are excluded [$\text{SDet}(S''[0])$ comes from the normalization]. The γ_i $(i = 1, \ldots, 8)$ are the collective coordinates, the flat directions related to the zero modes, and $J_{\text{zeros}}(\gamma_1, \ldots, \gamma_8)$ is the product of the Jacobians coming from the corresponding change of variables in the path integral (from usual to collective coordinates). In the SM there are eight zero modes: four translational (the collective coordinates being x_0, y_0, z_0, t_0, the coordinates of the center of the bounce), three related to $SU(2)$ "rotations" (the collective coordinates being the angles θ_1, θ_2, and θ_3), and finally, when the potential is taken as in Eq. (3) (where the mass term is neglected), one dilatation zero mode (the collective coordinate being the size R of the bounce). The complicated term in front of the exponential is often subdominant, although we will include it here.

For negative values of λ, the (Euclidean) equation of motion for the action (1) has nontrivial configuration solutions for the Higgs field (with $G_i = 0$), i.e. bounce solutions, which are solutions of the equation (r is the radial coordinate in $\mathbb{R}^4$)

$$\frac{d^2\phi}{dr^2} + \frac{3}{r}\frac{d\phi}{dr} - \frac{dV}{d\phi} = 0, \tag{5}$$

with boundary conditions

$$\phi(\infty) = 0, \tag{6}$$

$$\left.\frac{d\phi(r)}{dr}\right|_{r=0} = 0, \tag{7}$$

where $V(\phi)$ is

$$V(\phi) = \frac{\lambda}{4}\phi^4. \tag{8}$$

Note that Eq. (5) is also obtained by considering the restriction

$$S[\phi] = \int d^4x \left(\frac{1}{2}\partial_\mu\phi\partial_\mu\phi + V(\phi)\right) \tag{9}$$

of the action (1) when all the G_i vanish.

The family of bounce solutions to Eq. (5) is

$$\phi_b(r) = \sqrt{\frac{8}{|\lambda|}}\frac{R}{r^2 + R^2}, \tag{10}$$

and is parametrized by R, the size of the bounce $(0 < R < \infty)$.

For negative values of λ, the action (9) is scale invariant, so that all these configurations, irrespectively of the size R, have the same value of the action, namely

$$S[\phi_b] = \frac{8\pi^2}{3|\lambda|}. \tag{11}$$

From Eq. (10), we see that R and $\phi_b(0)$ [the maximal value of $\phi_b(r)$] are related by

$$R = \sqrt{\frac{8}{|\lambda|}}\frac{1}{\phi_b(0)} \tag{12}$$

and that R is nothing but that value of r such that

$$\phi_b(R) = \frac{1}{2}\phi_b(0). \tag{13}$$

In Fig. 2, we have sketched the potential. Note that the tunneling does not lead directly to the other side of the barrier. This is because of the gradient terms (surface tension for a thin-walled bubble), which require the bubble to gain volume energy. The point at the tip of the arrow is $\phi_b(0)$. The value of $\phi_b(0)$ can, in principle, be substantially larger than the point of the instability, and we will shortly see that this does, in fact, occur.

Going back to Eq. (4), we note that the integration over the center of the bounce (the four translational zero modes) can be immediately performed and gives the four-volume factor $\Omega = VT_U$ (V and T_U are the volume and the age of the Universe, respectively), which in our case is $\Omega = T_U^4$.

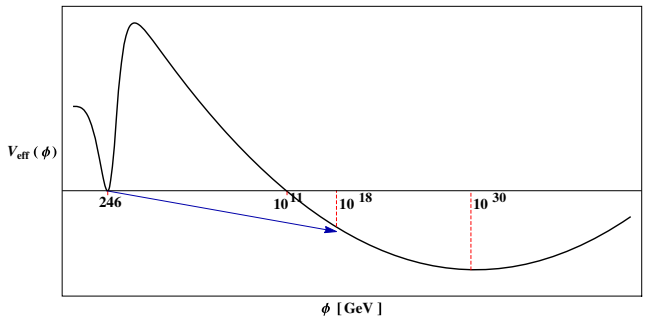

FIG. 2 (color online). The potential in the Standard Model, for $M_H = 125.7$ GeV and $M_t = 173.34$ GeV, is sketched (figure not to scale). The potential goes negative at a scale of 10^{11} GeV and reaches a new minimum at roughly 10^{30} GeV. The tunneling through the barrier goes from the base of the arrow [$\phi(r = \infty)$] to the tip [$\phi(0)$], which turns out to be close to or above the Planck scale.

The same is true for the integration over the angular $SU(2)$ variables (θ_1, θ_2, θ_3), which provides a factor $16\pi^2$.

Finally, concerning the integration in the remaining collective coordinate, the bounce size R, we note that, although the value of S is the same for all bounce sizes, R, quantum fluctuations break the degeneracy, and only one value of R, say R_M, saturates the path integral.

Therefore, from Eq. (4) for the tunneling probability, we can immediately write the tunneling time as

$$\tau = \left[\frac{R_M^4}{T_U^4} e^{\frac{8\pi^2}{3|\lambda(\mu)|}}\right] \times [e^{\Delta S}] \times T_U, \tag{14}$$

where we have used Eq. (11) for $S[\phi_b]$, and ΔS corresponds to quantum fluctuations, to be discussed shortly,

$$\Delta S = -\ln\left(\frac{16\pi^2}{R^8} J_{\rm trans} J_{SU(2)} J_{\rm dil} \left|\frac{\mathrm{SDet}'(S''(\phi_b))}{\mathrm{SDet}(S''(0))}\right|^{-1/2}\right)_{R=R_M}, \tag{15}$$

the Jacobian factor of Eq. (4) being split into the product of the three Jacobians related to the translation, dilatation, and $SU(2)$ zero modes (in Appendix A these Jacobian factors, together with the determinants, are computed).

Crucial to our analysis is the knowledge of the running of the quartic coupling $\lambda(\mu)$, to be solved together with the coupled Renormalization Group (RG) equations for the other SM couplings. We have used the RG equations up to the next-to-next-to-leading order. The beta functions and the boundary conditions up to this order have recently been worked out and are presented in [22,43–45].

By considering the RG equations for $\lambda(\mu)$, we see that the instability of the kind shown in Fig. 2 occurs when $\lambda(\mu)$ hits zero and then becomes negative. This is the case when the electroweak vacuum is metastable. For sufficiently large values of μ, $\lambda(\mu)$ saturates to a constant negative value. As for the renormalization scale $\mu_{\rm ren}$, it is convenient to choose $\mu_{\rm ren} \sim 1/R_M$. This is the value of $\lambda(\mu)$ to be used in Eq. (14). For $M_H = 127.5$ GeV and $M_t = 173.34$ GeV, we find

$$R_M \sim 1.87 \times 10^{-17}\ \mathrm{GeV}^{-1} = 224.5 M_P^{-1} \tag{16}$$

and

$$\lambda(1/R_M) = -0.01345, \tag{17}$$

which in turn gives

$$S[\phi_b] = 1956.54. \tag{18}$$

Inserting Eqs. (16) and (18) into Eq. (14), a first estimate of τ can be obtained by considering the classical (tree level) contributions only, i.e. by neglecting the quantum fluctuations (the term $e^{\Delta S}$). We find that

$$\tau_{\rm tree} \sim 10^{613} T_U. \tag{19}$$

At tree level, we already see that the electroweak vacuum lifetime τ turns out to be enormously larger than the age of the Universe, thus justifying the so-called metastability scenario: the electroweak vacuum is metastable but its lifetime is much larger than the age of the Universe. This is why the allowed region in Fig. 1 is so far from the line where the lifetime is the age of the Universe.

The next step is the inclusion of the quantum fluctuations. In Eq. (14), the contribution of the fluctuation determinant is given by the factor $e^{\Delta S}$. More precisely, each of the different sectors of the theory (Higgs, gauge, Goldstone, top) provides a contribution to ΔS, which then takes the form

$$\Delta S = \Delta S_H + \Delta S_t + \Delta S_{gg}, \tag{20}$$

where ΔS_H is the loop contribution from the Higgs sector, ΔS_t the contribution from the top sector, and ΔS_{gg} the one from the gauge and Goldstone sectors.

In Appendix A the computation of the different ΔS_i is shown. Here we present the results in the table below

	Loop contributions to τ
$e^{\Delta S_H}$	10^{-7}
$e^{\Delta S_t}$	10^{-19}
$e^{\Delta S_{gg}}$	10^{68}

Collecting the different multiplicative contributions to τ listed above, we finally have

$$\tau \sim 10^{655} T_U. \tag{21}$$

Despite the enormous difference in magnitudes between (19) and (21), it seems appropriate to quantify the distance between the classical and the quantum corrected estimates of τ by noting that in terms of orders of magnitudes, the

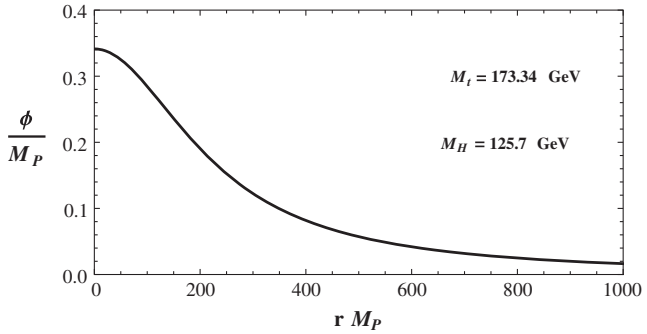

FIG. 3. Profile of the bounce solution that enters in the computation of the electroweak vacuum lifetime τ for $M_H = 125.7$ GeV and $M_t = 173.34$ GeV, the present central experimental values of M_H and M_t. The value of the field at the center of the bounce ($r = 0$) is $\phi_b(0) = 0.34 M_P$, very close to the Planck scale.

exponent 655 in (21) provides a 6% correction to the exponent 613 in (19). In this sense, even the tree level result (19) gives, in this framework, a "good" estimate of τ.

What we have just seen is that, even after the inclusion of the quantum fluctuation corrections, the lifetime of the electroweak vacuum τ turns out to be enormously larger than the age of the Universe, and this seems to give support to the metastability scenario. As explained in the Introduction, a more complete study of electroweak vacuum stability can be done in terms of the Higgs and top masses M_H and M_t. In Fig. 1, the corresponding SM phase diagram in the M_H-M_t plane is shown.

We now move to consider one of the key points of this paper, by turning our attention to the profile of the bounce. As we said above, because of the removal of the degeneracy from quantum fluctuations, the path integral for the computation of τ is saturated by only one of the bounces, with a specific value of the size R, R_M. For $M_H = 125.7$ GeV and $M_t = 173.34$ GeV, R_M is given in Eq. (16). Moreover, the value of the quartic coupling for the same values of M_H and M_t is given in Eq. (17). Then, from Eq. (10), we can determine the profile of the bounce that enters the evaluation of τ. The result is given in Fig. 3. We have also shown the profiles for different values of M_H and M_t in Fig. 4.

Looking at these results, we see that the value of the field at the center of the bubble, $\phi_b(r = 0)$, is dangerously close to the Planck scale. One can then suspect that Planck scale effects might be significant, even though the potential becomes unstable at a scale of roughly $10^{-8} M_P$, i.e. much below M_P. In this respect, it is important to note that the Planck mass never entered into our calculation, and we have simply scaled ϕ and r in terms of M_P, instead of GeV and GeV^{-1}, respectively.

The key point that emerges from inspecting these bounce profiles (Figs. 3 and 4), then, is that the value of the field at the center of the bubble can be not only substantially larger than the instability scale, but actually so close to M_P that Planck scale effects can be expected to affect the tunneling rate. In order to investigate this question, we will now add Planck scale operators to the potential and redo the calculation. We will see in the next section that the results (19) and (21) on the electroweak vacuum lifetime and the phase diagram of Fig. 1 can be dramatically modified.

III. BOUNCES AND NEW PHYSICS

In order to study the impact of new physics interactions at the Planck scale on the electroweak vacuum lifetime τ, following [39–41], we consider a simple modification of the theory by adding to the quartic potential (with negative λ) of the previous section two higher powers of the scalar field

$$V_{\text{new}}(\phi) = \frac{\lambda}{4}\phi^4 + \frac{\lambda_6}{6M_P^2}\phi^6 + \frac{\lambda_8}{8M_P^4}\phi^8. \qquad (22)$$

The goal of the present work is not that of studying specific models. Our aim is rather to show that the presence of new physics at the Planck scale is far from being harmless in the evaluation of the electroweak vacuum

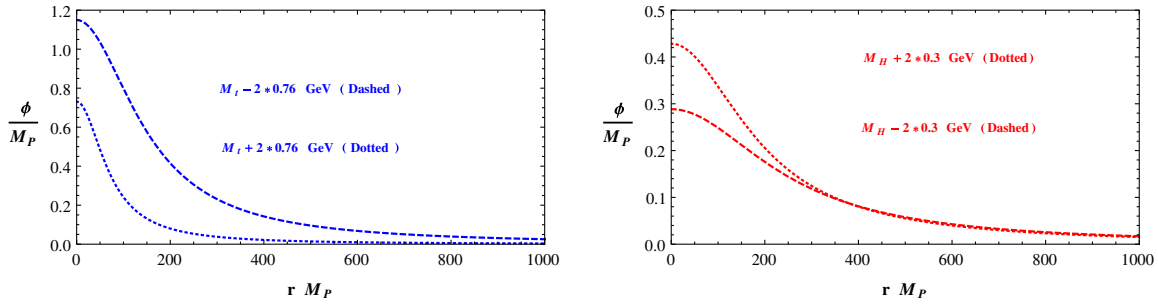

FIG. 4 (color online). Profile of the bounce solution that enters in the computation of the electroweak vacuum lifetime τ for values of M_H and M_t slightly different from those of Fig. 3. Actually, $\pm 2\sigma$ (current experimental errors) for M_t in the left panel (with M_H kept fixed to the central value $M_H = 125.7$ GeV), and $\pm 2\sigma$ (current experimental errors) for M_H in the right panel (with M_t kept fixed to the central value $M_t = 173.34$ GeV). As in Fig. 3, the values of the field at the center of the bounce, $\phi_b(0)$, turn out to be very close to the Planck scale, sometimes even above this scale.

lifetime. The choice of the potential (22) is well suited for this purpose. As a demonstration of a model in which this potential arises as an effective field theory (without, to leading order in the couplings, ϕ^{10} or higher terms), in Appendix C we have given an example from a minimal SU(5) model, in which M_P is replaced by the unification scale. This shows that it is very easy to have λ_6 and λ_8 of $O(1)$. In order to have a stable potential, λ_8 has to be taken positive, while λ_6 can have both signs. In the toy minimal SU(5) model that we look at in Appendix C this happens automatically.

In contrast with the previous section, with the potential (22) we cannot find analytical solutions to the Euclidean equation of motion (5). Moreover, the scale invariance of the action (9) is lost. However, when $\phi \ll M_P$ and the coupling constants λ_6 and λ_8 have natural $O(1)$ values, (22) is well approximated by (8). Under these conditions, the new action is *almost* scale invariant and the configurations (10) turn out to be good *approximate solutions* even for $V_{\rm new}(\phi)$. Note that as long as we limit ourselves to consider bounces of "large size" (large with respect to $1/M_P$), even in the presence of the higher order operators ϕ^6 and ϕ^8, the configurations (10) are (quasi-) solutions to the Euclidean equation of motion (a result to be expected).

In the computation of the tunneling time, then, these configurations have to be taken into account. We will come back to this point at the end of this section. But for now, let us look for the existence of exact bounce solutions to the Euclidean equation of motion (5) with the potential (22). Although we cannot rely on analytical tools, with the help of forward-backward shooting techniques [46], we can search for numerical solutions.

For our purposes, it is useful to rescale the radial coordinate r and the field ϕ by defining the dimensionless coordinate x and the dimensionless field φ in terms of Planck mass units

$$x = M_P r, \tag{23}$$

$$\varphi(r) = \frac{\phi(x)}{M_P}. \tag{24}$$

Equation (5), with the potential (22), then becomes

$$\frac{d^2\varphi}{dx^2} + \frac{3}{x}\frac{d\varphi}{dx} - \lambda\varphi^3 - \lambda_6\varphi^5 - \lambda_8\varphi^7 = 0, \tag{25}$$

while the boundary conditions are

$$\varphi(\infty) = 0, \tag{26}$$

$$\left.\frac{d\varphi(x)}{dx}\right|_{x=0} = 0. \tag{27}$$

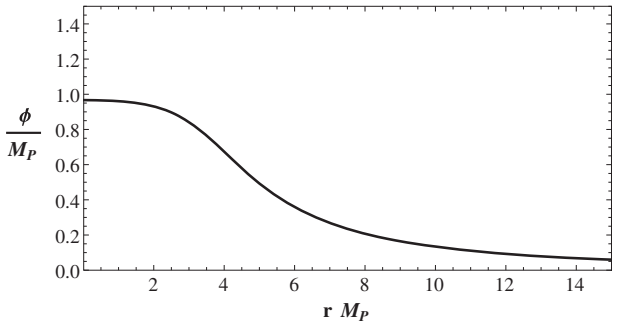

FIG. 5. Profile of the bounce solution found with the forward-backward method described in Appendix B for the potential of Eq. (22), with $\lambda = -0.01345$, $\lambda_6 = -2$, and $\lambda_8 = 2.1$.

In Appendix B, Eq. (25) is solved numerically with the help of forward-backward shooting methods. The profile $\varphi_{\rm bou}(r)$ of the bounce solution found with the help of the numerical procedure outlined in Appendix B is plotted in Fig. 5. Here we have somewhat arbitrarily chosen $\lambda_6 = -2$ and $\lambda_8 = 2.1$. This profile has to be compared with the bounce of Fig. 3, which is a solution obtained for the potential (8), i.e. in the absence of the higher order operators ϕ^6 and ϕ^8. Quite interestingly, the value of the field at the center of the bounce, $\phi_b(r = 0)$, is not much different from the values obtained for the case when the Planckian new physics operators ϕ^6 and ϕ^8 are absent (see Figs. 3 and 4).

Going back to dimensionful quantities, naming $\phi_{\rm bou}(r)$ the dimensionful counterpart of $\varphi_{\rm bou}(r)$ [see (23)] and defining the size $\bar{R}$ of this bounce according to (13), i.e. as that value of r such that

$$\phi_{\rm bou}(\bar{R}) = \frac{1}{2}\phi_{\rm bou}(0), \tag{28}$$

we obtain

$$\bar{R} \simeq 5.06 M_P^{-1}. \tag{29}$$

As for the corresponding action, from (9) and (22) we have

$$S[\phi_{\rm bou}] \simeq 82.09. \tag{30}$$

Note that this action is much, much less than the action in Eq. (18), implying that the lifetime of the electroweak vacuum is much, much smaller.

Let us pause for a moment to make some comments. The classical theory considered in the previous section is scale invariant. This is why we found an infinity of bounce solutions with all possible values of the size. The quantum fluctuations lifted the degeneracy, and the path integral was then dominated by a single bounce with a well defined size R_M. In the present case, the classical theory with potential (22) is no longer scale invariant. Accordingly, there is no degeneracy in the bounce size already at the classical level. Our numerical procedure, in fact, has shown that there is

only one bounce, with a well defined size $\bar{R}$, that solves the Euclidean equation of motion and satisfies the boundary conditions for the bounce. This removal of the degeneracy at the classical level certainly occurs whenever new physics interactions at the Planck (or, more generally, new physics) scale are included.

Having at our disposal $\bar{R}$ and $S[\phi_{\rm bou}]$, we are in the position to compute, according to (14), the tree-level contribution to τ, i.e. the contribution obtained neglecting the quantum fluctuation ($\Delta S = 0$),

$$\tau_{\rm tree} \sim \left[\frac{\bar{R}^4}{T_U^4} e^{S[\phi_{\rm bou}]}\right] T_U \sim 10^{-206} T_U. \tag{31}$$

Equation (31) is the key result. It has to be compared with Eq. (19) of the previous section. From this comparison we immediately see that the inclusion of new physics interactions at the Planck scale, already at the classical (tree) level, has produced a dramatic modification in the electroweak vacuum lifetime. A bona fide computation where new physics interactions at the Planck scale are explicitly taken into account has shown that they have a huge impact on the electroweak vacuum lifetime. Clearly, such values for λ_6 and λ_8 are phenomenologically unacceptable. This shows the importance of Planck scale operators on the metastability calculations and shows that the conventional diagram of Fig. 1 can be drastically changed by such operators.

It might be surprising that the Planck scale operators can have such a large effect. After all, while the value of the field at the center of the bubble is fairly close to the Planck scale, it is not substantially larger (and most of the field values throughout the bubble wall are substantially smaller) and thus one might expect $O(1)$ corrections, not the huge corrections we have seen. However, one must keep in mind that tunneling is a nonperturbative phenomenon. The tunneling rate is computed by looking for the bounce solution and then considering quantum fluctuations on top of that. While the latter are perturbative, and thus suppressed by inverse powers of the Planck scale, the former is not.

The potential (22) differs from the potential $\lambda\phi^4/4$, and the corresponding new saddle point $\phi_{\rm bou}$ provides a different nonperturbative contribution $e^{-S[\phi_{\rm bou}]}$ to the tunneling rate. The bounce $\phi_{\rm bou}(r)$ is a profile, not a localized configuration, defined in the whole range $r \in [0, \infty[$. Although $\phi_{bou}(r)$ looks similar to the profile $\phi_b(r)$ of the previous section, the difference between these two profiles provides the difference between the two exponentials $e^{-S[\phi_b]}$ (previous section) and $e^{-S[\phi_{bou}]}$ (this section), and these two numbers are exponentially decoupled.

As in the previous section, the next step consists of the inclusion of the quantum fluctuations. Once again, the contribution of the fluctuation determinant is given in terms of the factor $e^{\Delta S}$ and, as before, each of the different sectors of the theory (Higgs, gauge, Goldstone, top) provides a contribution to ΔS ($\Delta S = \Delta S_H + \Delta S_t + \Delta S_{gg}$). These are computed in Appendix A. Here we present the results in the table below

	Loop contributions to τ
$e^{\Delta S_H}$	10^{-9}
$e^{\Delta S_t}$	10^{-5}
$e^{\Delta S_{gg}}$	10^{8}

Collecting now the different multiplicative contributions listed above to the electroweak vacuum lifetime τ, we finally have

$$\tau \sim 10^{-212} T_U. \tag{32}$$

As before, we have an enormous difference between the tree level result (31) for τ and the quantum corrected one (32), but we again see that the bulk of the contribution to τ comes from the classical level, which, in this sense, provides a good estimate of τ.

In the case that we have just considered, the electroweak vacuum lifetime τ turns out to be enormously shorter than the age of the Universe, thus showing that the metastability scenario is far from being a generic feature of theories which allow for the SM to be valid all the way up to the Planck scale. The expectations and arguments of [18,21,22] are simply not fulfilled.

Clearly, in the light of the above results, the SM phase diagram in the M_H-M_t plane of Fig. 1 no longer holds. For the case that we have considered, for instance, the instability line is tremendously lowered and the big dot in the figure, corresponding to $M_H = 125.7$ GeV and $M_t = 173.34$ GeV, lies within the instability region. See [41], where new phase diagrams of this kind are plotted.

Before ending this section, we would like to come back to the question of the existence of other bounce solutions and/or of configurations that are quasisolutions. In principle, if, in addition to the solution found above, other solutions or quasisolutions are present, they could contribute to τ and the result (32) should be revisited. However, this is not the case here. As we have just seen, in fact, the action related to the solution $\phi_{\rm bou}(r)$ found above, is $S[\phi_{\rm bou}] \sim 80$ [see (30)], while for the (quasi-)solutions mentioned at the beginning of this section, the action is [see (18)] $S[\phi_b] \sim 1800$. This means that the contribution of the latter is enormously (exponentially) suppressed as compared to the contribution of $\phi_{\rm bou}(r)$.

IV. ANALYTICAL APPROXIMATIONS

We would like to compare now the results of the previous sections with those obtained in [39], where the presence of new physics interactions was studied with the help of an approximation for the potential $V_{\rm new}(\phi)$ in (22) that made it possible to get analytic solutions for the bounces.

The solid line in Fig. 6 shows the plot of the potential (22) with $\lambda = -0.01435$, $\lambda_6 = -2$, and $\lambda_8 = 2.1$. Up to the

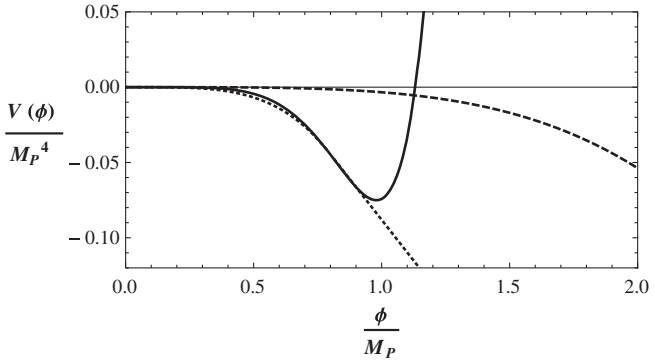

FIG. 6. The solid line shows the potential $V_{\rm new}(\phi)$ of Eq. (22) with $\lambda=-0.01345$, $\lambda_6=-2$, and $\lambda_8=2.1$. The dotted line is the plot of the approximation to $V_{\rm new}(\phi)$ given in Eq. (33), with $\eta\simeq 0.7912M_P$ (determined self-consistently in the text), $\lambda_{\rm eff}=\lambda+\frac{2}{3}\lambda_6\frac{\eta^2}{M_P^2}+\frac{1}{2}\lambda_8\frac{\eta^4}{M_P^4}=-0.4366$, and $\gamma=-\lambda_{\rm eff}\eta^3(\lambda\eta^3+\lambda_6\frac{\eta^5}{M_P^2}+\lambda_8\frac{\eta^7}{M_P^4})^{-1}=-0.987$. As explained in the text, the latter provides a good approximation to $V_{\rm new}(\phi)$ for values of ϕ around η. The dashed line is the potential in the absence of new physics interactions ($\lambda_6=0$ and $\lambda_8=0$).

scale $\eta\simeq 0.7912M_P$ (that will be determined self-consistently in the following), $V_{\rm new}(\phi)$ is well approximated by an upside down quartic parabola, $V_{\rm new}(\phi)\simeq\frac{\lambda_{\rm eff}}{4}\phi^4$, with $\lambda_{\rm eff}=\lambda+\frac{2}{3}\lambda_6\frac{\eta^2}{M_P^2}+\frac{1}{2}\lambda_8\frac{\eta^4}{M_P^4}$. For $\phi>\eta$, $V_{\rm new}(\phi)$ bends down creating a new minimum at $\phi_{\rm min}\simeq 0.979M_P$. Therefore, for values of ϕ larger than (but close to) η, $\phi\gtrsim\eta$, $V_{\rm new}(\phi)$ can be linearized and we get $V_{\rm new}(\phi)=[\frac{\lambda_{\rm eff}}{4}\eta^4-\frac{\lambda_{\rm eff}\eta^3}{\gamma}(|\phi|-\eta)]$, with $\gamma=-\lambda_{\rm eff}\eta^3(\lambda\eta^3+\lambda_6\frac{\eta^5}{M_P^2}+\lambda_8\frac{\eta^7}{M_P^4})^{-1}$.

The previous approximations can be included in a single expression. Indeed, the potential $V_{\rm new}(\phi)$, for values of ϕ around η, can finally be written as

$$V_{\rm new}(\phi)\simeq\frac{\lambda_{\rm eff}}{4}\phi^4\theta(\eta-|\phi|)+\left[\frac{\lambda_{\rm eff}}{4}\eta^4-\frac{\lambda_{\rm eff}\eta^3}{\gamma}(|\phi|-\eta)\right]\theta(|\phi|-\eta). \quad (33)$$

The equation of motion possesses the bounce solution

$$\phi_b(r)=\begin{cases}2\eta-\eta^2\sqrt{\frac{|\lambda_{\rm eff}|}{8}}\frac{r^2+\bar R^2}{\bar R} & 0<r<\bar r\\ \sqrt{\frac{8}{|\lambda_{\rm eff}|}}\frac{\bar R}{r^2+\bar R^2} & r>\bar r\end{cases}, \quad (34)$$

where

$$\bar r=\sqrt{\frac{8\gamma}{\lambda_{\rm eff}\eta^2}(1+\gamma)},\qquad \bar R=\sqrt{\frac{8}{|\lambda_{\rm eff}|}\frac{\gamma^2}{\eta^2}}, \quad (35)$$

$\bar R$ being the size of the bounce [see Eq. (34)], and the action is

$$S[\phi_b]=(1-(\gamma+1)^4)\frac{8\pi^2}{3|\lambda_{\rm eff}|}. \quad (36)$$

From Eq. (31) we see the expression for the main contribution to the tunneling time. Therefore, in the approximation that we are considering, the tunneling time is obtained maximizing the expression

$$\mathcal{T}(\eta)=\frac{\bar R(\eta)^4}{T_U^4}e^{S[\phi_b(\eta)]} \quad (37)$$

with respect to η. This in turn determines the value of η appearing in Eq. (33).

By considering the values $\lambda=-0.01345$, $\lambda_6=-2$, and $\lambda_8=2.1$ of the example in Fig. 6, we find $\eta=0.7912M_P$. The dotted line in this figure is the plot of the approximation in Eq. (33) for the potential $V_{\rm new}(\phi)$ for the above value of η. We immediately see that this is an excellent approximation for the potential for value of ϕ close to η. In this respect, we should note that for the purposes of computing the bounce, this is the only region of interest [47].

The profile of the bounce solution found with this approximation is shown in Fig. 7 and has to be compared with the bounce obtained numerically, shown in Fig. 5. Moreover, the tunneling time under this approximation turns out to be

$$\tau\sim 10^{-215}T_U, \quad (38)$$

which is a quite good estimate for τ, to be compared with the exact numerical result of Eq. (31).

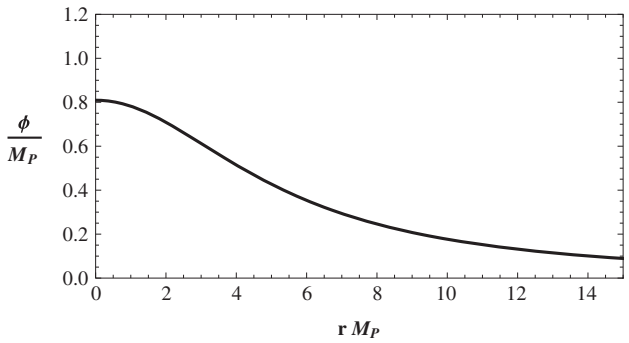

FIG. 7. The analytical bounce solution, Eq. (34), when $V_{\rm new}(\phi)$ is approximated as in Eq. (33), for the values of the parameters considered in the text (see also Fig. 6). In particular, from Eq. (35), we have $\bar r=0.61M_P^{-1}$, and for the bounce size, $\bar R=5.33M_P^{-1}$.

V. CONCLUSIONS

During the early discussions of the stability of the Standard Model Higgs potential, the top quark and Higgs masses were completely unknown. It is remarkable that the values of these masses turn out to lead to a corner of parameter space in which the stability, metastability, and instability regions are so close together. As a result, calculations need to be carried out to higher precision in order to determine the ultimate fate of our vacuum.

Although these calculations have been done, it was shown in Refs. [39–41] that higher dimensional Planck scale operators, neglected in previous calculations, could have an enormous effect on the tunneling rate, and thus on the lifetime of the Standard Model vacuum. As a result, predictions of the fate of our vacuum without knowledge of these operators cannot reliably be made.

Neglecting Planck scale operators would seem to be completely reasonable, since the electroweak vacuum becomes unstable at a scale of 10^{11} GeV, far, far below the Planck scale. In this paper we have pointed out two reasons why they are still important (and can dominate the tunneling rate). First, when the Higgs field tunnels through a potential barrier (in more than one dimension), the value of the field at the center of the bubble is much, much bigger than the location of the instability. This is because additional vacuum energy is needed to overcome the gradient terms in the Higgs Lagrangian; this is nothing other than needing a large volume energy difference to overcome surface tension. In the SM, this results in the value of the field at the center of the bubble being roughly 10^7 times the value at the instability, which happens to be close to the Planck scale. Second, tunneling is an inherently nonperturbative process, and thus one's naive expectation that higher dimensional operators will have effects which are strongly Planck-scale suppressed may not be valid. All one can do is to redo the calculations including higher dimensional operators to see if their effect is significant. This was done in Refs. [39–41], where it was shown that they can have a huge effect.

These previous calculations made several simplifying assumptions. They used an analytic approximation to the Higgs potential and for the tunneling rate. While this is a reasonable way to estimate the size of the Planck scale operators, a more precise calculation is needed. In this paper, we have improved on the previous results in several ways. We have used fully numerical techniques to solve for the bounce action and the tunneling rate, without the earlier analytic approximations. We have included not only Higgs loop contributions to the tunneling rate, but the contributions of the other fields as well. In addition, a toy $SU(5)$ model shows that the type of higher dimensional operators with the given coefficients is completely reasonable. The results confirm the earlier calculations and show that Planck scale operators do, in fact, have a huge effect on the tunneling rate. Only with knowledge of these higher dimensional operators can the fate of our vacuum be known.

There are many other situations in which these operators can have a large effect. As noted in Ref. [41], the Higgs inflation scenario would be drastically altered. In fact, one generally can be concerned about the basic slow-roll inflation scenario. It is always assumed that the inflaton rolls down the potential, following the classical equations of motion. However, while it is rolling, it could tunnel through, changing the inflation scenario completely; higher dimensional operators can drastically alter the tunneling rate, making this possibility much more likely. Clearly, there are many potential applications of this scenario.

Finally, as the higher dimensional Planck scale operators could have an enormous impact on the stability phase diagram of the Standard Model, the common expectation that more precise measurements of the top and Higgs masses would allow one to discriminate between whether our vacuum is stable or metastable (or critical) turns out to be unjustified. Without the knowledge of the (Planck scale) new physics interactions, no conclusion on the electroweak vacuum stability can be drawn, a better knowledge of M_t and M_H being of no help in that respect [41].

ACKNOWLEDGMENTS

One of us (V. B.) would like to thank M. Consoli, G. Degrassi, G. Giudice, G. Isidori, M. Krawczyk, T. Gehrmann, and D. Zappalà for several helpful discussions. The work of M. S. was initiated at the Scalars 2013 Workshop in Warsaw, Poland, and was then supported by the National Science Foundation under Grant No. NSF-PHY-1068008. The opinions and conclusions expressed herein are those of the authors and do not represent the National Science Foundation.

APPENDIX A FLUCTUATION DETERMINANTS

In this Appendix we outline the computation of the quantum fluctuation contribution to the electroweak vacuum lifetime from the different sectors of the Standard Model; see Eqs. (14), (15), and (20) in the text.

If we denote with $\chi_r(x)$ all of the SM fields (the index "r" indicates the different fields), the semiclassical approximation to the path integral for the computation of the tunneling rate is obtained by expanding around the configuration $\chi_r^b(x)$ that consists of a collection of zeros, except for the case when the index r indicates the Higgs field, in which case $\chi_r^b(x) = \phi_b(x)$, the bounce solution. Let us then indicate the saddle point as $\chi^b(x)$.

The tunneling rate is computed by performing a saddle point expansion of the transition amplitude around $\chi^b(x)$ according to

$$\chi(x) = \chi^b(x) + \sum_j c_j \eta_j(x), \tag{A1}$$

where $\eta_j(x)$ is a complete set of orthonormal eigenfunctions of the second variation operator

$$(S''[\chi_b])_{rs} = \left.\frac{\delta^2 S[\chi]}{\delta\chi_r(x)\delta\chi_s(y)}\right|_{\chi=\chi^b}, \tag{A2}$$

where the r and s indices run over all the sectors of the model.

The computation of the tunneling rate is complicated by the presence of some zero eigenvalues in the spectrum of the operator $S''[\chi^b]$ and of a negative eigenvalue. The zero modes are related to symmetries of the classical action with respect to four translations (in Euclidean space-time), to dilatation (a symmetry that is broken by quantum effects), and to three $SU(2)$ global rotations. With reference to the two cases treated in the text, where we have considered the case of the Standard Model alone with the quartic potential, and the case where the SM is modified due to the presence of new physics interactions, higher powers of the scalar field, the dilatation symmetry of the classical action is present only in the first case.

In the functional space, these are flat directions, and we take care of them with the help of eight collective coordinates (seven in the case that the dilatation invariance is absent). Let us indicate with γ_i (for $i = 1, \ldots, 8$) these collective coordinates: the spatial coordinates x_0^μ of the center of the bounce, the three Euler angles θ_i of the group space of $SU(2)$, and the size of the bounce R.

Actually, the instanton (bounce) size R is a collective coordinate only when the theory is scale invariant (dilatation symmetry). This is the case for the SM (when the scalar mass term is neglected). When new physics interactions as those appearing in the potential (22) are taken into account, the dilatation symmetry is lost, the collective coordinate R is missing, and we have only seven zero modes.

In the following we will treat the case when all of the eight symmetries are present, bearing in mind that we are also interested in the case when dilatation symmetry is lost. Therefore the superdeterminant of the fluctuation operator is modified according to

$$\begin{aligned}&(\mathrm{SDet}(S''(\chi_b)))^{-1/2}\\ &\to \frac{1}{2}(2\pi)^{-8/2}\int\prod_{r=1}^{8} d\gamma_r \det\left(\frac{\partial c_i}{\partial\gamma_j}\right)|\mathrm{SDet}'(S''(\chi_b))|^{-1/2},\end{aligned} \tag{A3}$$

where the γ_i are the collective coordinates mentioned above that allow one to perform the integration along the flat directions exactly. The contribution of the zero modes is encoded in the Jacobian. The factor $(2\pi)^{-8/2}$ arises to compensate the missing Gaussian integrations, and the negative mode provides the factor $1/2$ and the absolute value in the determinant [38].

Let us define the $SU(2)$ multiplet $\Phi_b(x)$ as

$$\Phi_b(x) = \frac{1}{\sqrt{2}}\begin{pmatrix} 0 \\ \phi_b(x)\end{pmatrix}. \tag{A4}$$

The Jacobian $J = (2\pi)^{-4}\det(\frac{\partial c_i}{\partial\gamma_j})$ is written in terms of the norm of the eight linearly independent zero modes $\frac{\partial\Phi_b(x,\gamma)}{\partial\gamma_j}$ and turns out to be

$$J = \det\begin{pmatrix} \frac{1}{2\pi}\int d^4x\,\partial_\mu\Phi_b^\dagger\partial_\nu\Phi_b & 0 & 0 \\ 0 & \frac{1}{2\pi}\int d^4x\,\frac{\partial}{\partial R}\Phi_b^\dagger\frac{\partial}{\partial R}\Phi_b & 0 \\ 0 & 0 & \frac{1}{2\pi}\int d^4x\,\frac{\partial}{\partial\theta_i}\Phi_b^\dagger\frac{\partial}{\partial\theta_j}\Phi_b\end{pmatrix}^{1/2}. \tag{A5}$$

Since the above matrix has a block diagonal form, J can be expressed as the product of J_{trans}, the contribution of the translational zero modes, times $J_{SU(2)}$, the contribution of the zero modes related to the $SU(2)$ global symmetry, times J_{il}, the contribution of the dilatation zero mode.

The Jacobian J_{trans} is given by

$$J_{\mathrm{trans}} = (2\pi)^{-2}\int d^4x\prod_{\mu=1}^{4}[(\partial_\mu\Phi_b^\dagger\partial_\mu\Phi_b)]^{1/2} = \frac{S[\phi_b]^2}{4\pi^2}. \tag{A6}$$

As for the Jacobian $J_{SU(2)}$, let us consider it in conjunction with the integration in the three corresponding collective coordinates

$$\begin{aligned}&\int\prod_{r=1}^{3} d\theta_r J_{SU(2)}\\ &\quad= \int\prod_{r=1}^{3} d\theta_r \det\left(\frac{1}{2\pi}\int d^4x\,\frac{\partial}{\partial\theta_i}\Phi_b^\dagger\frac{\partial}{\partial\theta_j}\Phi_b\right)^{1/2},\end{aligned} \tag{A7}$$

where $\theta_1 \in [0, 2\pi]$, $\theta_2 \in [0, \pi]$, and $\theta_3 \in [0, 2\pi]$.

We can obtain an expression that is the product of a measure term invariant under the global $SU(2)$ transformation times a quantity that does not depend on the variables θ_i. To this end, we multiply and divide the expression in Eq. (A7) for $\sin\theta_2$. Then, by further multiplying and dividing the same expression for R^3, we can also extract the dimensions from $J_{SU(2)}$ thus obtaining

$$\int d^3\theta J_{SU(2)} = \int d^3\theta \sin\theta_2 R^3 J'_{SU(2)}, \tag{A8}$$

where the new dimensionless Jacobian $J'_{SU(2)}$ is

$$J'_{SU(2)} = \frac{1}{R^3 \sin\theta_2} \det\left(\frac{1}{2\pi}\int d^4x \frac{\partial}{\partial\theta_i}\Phi_b^\dagger \frac{\partial}{\partial\theta_j}\Phi_b\right)^{1/2}, \tag{A9}$$

and the invariant measure is $d^3\theta \sin\theta_2$.

$J'_{SU(2)}$ can now be made explicit by writing Φ_b in terms of a generic $SU(2)$ transformation applied to Φ_b^0 defined as $\Phi_b^0 \equiv \Phi_b(x, x_0, R, \theta_i = 0)$. By replacing then

$$\Phi_b = e^{i\theta_1 T_1} e^{i\theta_2 T_2} e^{i\theta_3 T_3} \Phi_b^0 \tag{A10}$$

in Eq. (A9) and performing some algebraic manipulations we get

$$\begin{aligned} J'_{SU(2)} &= \frac{1}{R^3} \det\left(\frac{1}{2\pi}\int d^4x \Phi_b^{0\dagger} T_i^\dagger \cdot T_j \Phi_b^0\right)^{1/2} \\ &= \frac{1}{R^3}\left[\frac{1}{2\pi}\int d^4x \phi_b^2\right]^{3/2}, \end{aligned} \tag{A11}$$

where T_i (for $i = 1, 2, 3$) is the real representation of the $SU(2)$ generators.

Finally the contribution of the dilatational zero mode $J_{\rm dil}$ is

$$J_{\rm dil} = \left(\frac{1}{2\pi}\int d^4x \left(\frac{\partial\phi_b}{\partial R}\right)^2\right)^{1/2}. \tag{A12}$$

Bearing in mind that the integration over the $SU(2)$ angular variables provides a factor $16\pi^2$ and that the volume factor $\int d^4x_0$ is 4 times the time of the universe T_U, referring to Eq. (4) in the text, we find that the tunneling rate T_U/τ for unit volume and time is

$$\begin{aligned} p = {} & e^{-S[\chi_b]} 16\pi^2 V T_U \\ & \times \int dR R^3 J_{\rm trans} J_{SU(2)} J_{\rm dil} \left|\frac{\mathrm{SDet}'(S''(\chi_b))}{\mathrm{SDet}(S''(0))}\right|^{-1/2}, \end{aligned} \tag{A13}$$

where T_U is the age of the Universe and V the volume ($V = T_U^3$). Note that the dimensional factor $T_U^4 \int dR R^3$ is compensated by the dimension of the ratio $\mathrm{SDet}'(S''(\chi_b))/\mathrm{SDet}(S''(0))$.

Finally, we recall that the fluctuation determinant breaks the scale invariance, so that only one of the bounces, with a specific value of the size R, dominates the above integral. Referring again to the notation introduced in the text, we indicate with R_M this value of R and we have

$$\begin{aligned} \frac{\tau}{T_U} = {} & \frac{R_M^4}{T_U^4} e^{S[\phi_b]} \\ & \times \left(\frac{16\pi^2}{R^8} J_{\rm trans} J_{SU(2)} J_{\rm dil} \left|\frac{\mathrm{SDet}'(S''(\phi_b))}{\mathrm{SDet}(S''(0))}\right|^{-1/2}\right)^{-1}_{R=R_M}, \end{aligned} \tag{A14}$$

from which we immediately get Eq. (15) in the text.

It is worth stressing here that when the dilatation symmetry is absent, as is the case for the modified potential considered in this paper, where new physics interactions are added to the usual SM potential [see Eq. (22) in the text], the above formula has to be modified in the following three aspects. The size R of the bounce that appears in (A14) is no longer the result of the maximization of the integrand function, but comes directly from the equation of motion (the action is not scale invariant already at the classical level, so we have only one bounce, no degeneracy). For the same reason, $J_{\rm dil}$ is absent and the factor R^{-8} becomes R^{-6}.

The next step concerns the evaluation of the ratio

$$\left|\frac{\mathrm{SDet}'(S''(\chi_b))}{\mathrm{SDet}(S''(0))}\right|^{-1/2}, \tag{A15}$$

with contributions from the different sectors of the Standard Model. More specifically, we have to compute the contribution from the Higgs field ϕ, the three Goldstone bosons G_i (for $i = 1, 2, 3$), the four gauge fields A_μ^a (for $a = 1, 2, 3, 4$), the four corresponding ghost fields c_a, and the heaviest matter contribution, i.e. the contribution from top quark ψ (the contribution of the other fermion fields are far less important and can be neglected).

In the following we will see that the S'' operator takes block diagonal form, each block being related to one of the following three different sectors: Higgs, top, and gauge + Goldstone. To this end, we write down the different contribution to the EW Lagrangian and extract its quadratic part in the fields, the only part that is relevant for the computation of the fluctuations around the bounce.

The action of the scalar sector of the model, Eq. (1) is usually written in terms of the $SU(2)$ doublet of Eq. (2) (here we write $\phi = \phi_b + H$),

$$\Phi = \begin{pmatrix}\phi^+ \\ \phi^0\end{pmatrix} = \frac{1}{\sqrt{2}}\begin{pmatrix}-i(G_1 - iG_2) \\ \phi_b + H + iG_3\end{pmatrix}. \tag{A16}$$

However, for our purposes it is useful to consider the real four dimensional representation of the $SU(2) \times U(1)$ group acting on the scalar multiplet $\phi_i = (G_1, G_2, G_3, \phi_b + H)$, so that by adding the interaction term between the scalars and the gauge fields we get

$$\mathcal{L}_{\rm scalar} = \frac{1}{2}(D_\mu\phi_i)^2 + V(\phi_i^2) = \frac{1}{2}(\partial_\mu\phi_i)^2 + V(\phi_i^2) + \frac{1}{2}g_a^2(T^a)_{ji}(T^b)_{jk}\phi_i\phi_k A_\mu^a A_\mu^b + g_a(T^a)_{ij}\partial_\mu\phi_i\phi_j A_\mu^a, \quad \text{(A17)}$$

where (with the mass term neglected, i.e. for large values of the scalar field)

$$V(\phi_i^2) = \frac{\lambda}{4}(\phi_i\phi_i)^2 \quad \text{(A18)}$$

when we consider the SM interactions only. When, on the contrary, we also take into account the presence of new physics interactions as those considered in Eq. (22), the potential takes the form

$$V(\phi_i^2) = \frac{\lambda}{4}(\phi_i\phi_i)^2 + \frac{\lambda_6}{6M_P^2}(\phi_i\phi_i)^3 + \frac{\lambda_8}{8M_P^4}(\phi_i\phi_i)^4. \quad \text{(A19)}$$

The computation of the fluctuation determinant in the presence of these additional terms presents quite nontrivial aspects. However, for the time being, we continue to write the formulas referring only to the potential of Eq. (A18), bearing in mind that they have to be modified by inserting the potential Eq. (A19) when we take into account the presence of new physics.

Note that in Eq. (A17) we have written the covariant derivative D_μ in terms of the 4×4 $SU(2)\times U(1)$ generators T^a ($a = 1, 2, 3, 4$), of the four gauge bosons A_μ^a, and of the gauge coupling g_a [that are g for $a = 1, 2, 3$ and g' for $a = 4$, i.e. the usual $SU(2)$ and $U(1)$ couplings, respectively] as

$$D_\mu = \partial_\mu + g_a T^a A_\mu^a. \quad \text{(A20)}$$

The quadratic part of Eq. (A17) is therefore given by

$$\mathcal{L}^{(2)}_{\rm scalar} = \frac{1}{2}(\partial_\mu\phi_b)^2 + \frac{\lambda}{4}\phi_b^4 + \frac{1}{2}(\partial_\mu H)^2 + \frac{3}{2}\lambda\phi_b^2 H^2 + \frac{1}{2}\sum_i(\partial_\mu G_i)^2 + \frac{\lambda}{2}\phi_b^2\sum_i G_i^2 + \frac{\phi_b^2}{8}(g^2A^{1\mu}A_\mu^1 + g^2A^{2\mu}A_\mu^2 + (g^2+g'^2)Z^\mu Z_\mu) + gA_\mu^1\phi_b\partial_\mu G_1 + gA_\mu^2\phi_b\partial_\mu G_2 + \sqrt{g^2+g'^2}Z^\mu\phi_b\partial_\mu G_3 + \frac{g}{2}\partial^\mu A_\mu^1\phi_b G_1 + \frac{g}{2}\partial_\mu A^{2\mu}\phi_b G_2 + \frac{\sqrt{g^2+g'^2}}{2}\partial_\mu Z^\mu\phi_b G_3, \quad \text{(A21)}$$

where the equation of motion $-\partial^2\phi_b + \lambda\phi_b^3 = 0$ has been used and we have rotated the gauge fields A_μ^3 and A_μ^4 according to the transformations

$$A_\mu^3 = \frac{1}{\sqrt{g^2+g'^2}}(gZ_\mu + g'A_\mu), \qquad A_\mu^4 = \frac{1}{\sqrt{g^2+g'^2}}(gA_\mu - g'Z_\mu). \quad \text{(A22)}$$

The kinetic term for the four gauge bosons is given by

$$\mathcal{L}_{\rm gauge,kin} = \frac{1}{4}F_{\mu\nu}^a F^{a\mu\nu}, \quad \text{(A23)}$$

where

$$F_{\mu\nu}^a = \partial_\mu A_\nu^a - \partial_\nu A_\mu^a + g_a f^{abc}A_\mu^b A_\nu^c. \quad \text{(A24)}$$

The f^{abc} are the structure constants of the group which are equal to ϵ^{abc} when all the indices take one of the values 1, 2, 3 and zero otherwise. The quadratic part in the gauge fields of the Lagrangian in Eq. (A23) is given by

$$\mathcal{L}^{(2)}_{\rm gauge,kin} = \frac{1}{2}\sum_{a=1}^4 A_\mu^a(-\partial^2\delta^{\mu\nu} + \partial^\mu\partial^\nu)A_\nu^a = \frac{1}{2}\sum_{i=1}^2 A_\mu^i(-\partial^2\delta^{\mu\nu} + \partial^\mu\partial^\nu)A_\nu^i + \frac{1}{2}A_\mu(-\partial^2\delta^{\mu\nu} + \partial^\mu\partial^\nu)A_\nu + \frac{1}{2}Z_\mu(-\partial^2\delta^{\mu\nu} + \partial^\mu\partial^\nu)Z_\nu, \quad \text{(A25)}$$

where again the rotation in Eq. (A22) is considered.

We use the R_ξ gauge fixing, so that the gauge fixing Lagrangian is written as

$$\mathcal{L}_{\rm gauge,fix} = \frac{1}{2\xi}(\partial_\mu A^{a\mu} + \xi g_a(T^a)_{ij}\phi_b^j(\phi^i - \phi_b^i))^2. \quad \text{(A26)}$$

The quadratic part of the Lagrangian in Eq. (A26) is

$$\mathcal{L}^{(2)}_{\rm gauge,fix} = -\frac{1}{2\xi}\sum_{i=1}^2 A_\mu^i\partial^\mu\partial^\nu A_\nu^i - \frac{1}{2\xi}A_\mu\partial^\mu\partial^\nu A_\nu - \frac{1}{2\xi}Z_\mu\partial^\mu\partial^\nu Z_\nu + \frac{\xi}{8}\phi_b^2(g^2(G_1^2+G_2^2) + (g^2+g'^2)G_3^2) + \frac{g}{2}\partial^\mu A_\mu^1\phi_b G_1 + \frac{g}{2}\partial_\mu A^{2\mu}\phi_b G_2 + \frac{\sqrt{g^2+g'^2}}{2}\partial_\mu Z^\mu\phi_b G_3. \quad \text{(A27)}$$

Note that the terms that mix the gauge and Goldstone fields in Eq. (A27), together with the analogous terms in Eq. (A21), give

$$-gA_\mu^1\partial^\mu\phi_b G_1 - g\partial_\mu A^{2\mu}\phi_b G_2 - \sqrt{g^2+g'^2}Z^\mu\partial_\mu\phi_b G_3. \tag{A28}$$

Moreover, the contribution to the determinant coming from the field A_μ in Eqs. (A21) and (A27) is the same as in the free case. Therefore, when the ratio of determinants is performed, these terms disappear.

In addition to the gauge fixing terms, the Fadeev-Popov quantization also requires the introduction of four additional ghost fields c^a (with the corresponding conjugate fields c_a^*), the Lagrangian being

$$\mathcal{L}_{\text{ghost}} = c_a^*[-\partial^\mu D_\mu^{ab} + \xi g_a^2(T^a\cdot\phi_b)\cdot(T^b\cdot\phi)]c_b, \tag{A29}$$

where the covariant derivative for the ghost fields is given by $D_\mu^{ac} = \partial_\mu\delta^{ac} + g_a f^{abc}A_\mu^b$. The quadratic part of (A29) is

$$\mathcal{L}^{(2)}_{\text{ghost}} = \sum_{i=1}^{2} c_i^*\left(-\partial^2 + \xi\frac{g^2}{4}\phi_b^2\right)c_i + c_3^*\left(-\partial^2 + \xi\frac{g^2+g'^2}{4}\phi_b^2\right)c_3 + c_4^*(-\partial^2)c_4. \tag{A30}$$

As in the case of the A_μ fields above, the ghost c_4 gives the same contribution as in the free case, and then it can be neglected.

Finally, for the fermions fields, the only relevant contribution comes from the top quark (all the other contributions being negligible). The quadratic part of the top Lagrangian, in the bounce background field, is then (g_t is the Yukawa top coupling and ψ the top field)

$$\mathcal{L}_F^{(2)} = \bar\psi\left(\partial\!\!\!/ + \frac{g_t}{\sqrt{2}}\phi_b\right)\psi. \tag{A31}$$

With all the above building blocks at our disposal, we are finally in the position to write the fluctuation operator $S''(\chi_b)$. It takes the block diagonal form

$$S''(\chi_b) = \begin{pmatrix} S_{HH} & 0 & 0 & 0 & 0 & 0 & 0 \\ 0 & 0 & S_{\psi\bar\psi} & 0 & 0 & 0 & 0 \\ 0 & S_{\bar\psi\psi} & 0 & 0 & 0 & 0 & 0 \\ 0 & 0 & 0 & S_{\tilde A^i\tilde A^i} & S_{\tilde A^i G^i} & 0 & 0 \\ 0 & 0 & 0 & S_{G^i\tilde A^i} & S_{G^iG^i} & 0 & 0 \\ 0 & 0 & 0 & 0 & 0 & 0 & S_{c_ic_i^*} \\ 0 & 0 & 0 & 0 & 0 & S_{c_i^*c_i} & 0 \end{pmatrix}, \tag{A32}$$

where $i = 1,2,3$ and we have set $\tilde A_\mu^i = (A_\mu^1, A_\mu^2, Z_\mu)$.

Since this matrix is block diagonal, SDet in Eq. (A15) becomes the product of the different determinants appearing in the different blocks, i.e. the product of the determinants of the operators

$$S''_H \equiv S_{HH}$$
$$S''_t \equiv \begin{pmatrix} 0 & S_{\psi\bar\psi} \\ S_{\bar\psi\psi} & 0 \end{pmatrix}$$
$$S''_{gg} \equiv \begin{pmatrix} S_{\tilde A^i\tilde A^i} & S_{\tilde A^i G^i} \\ S_{G^i\tilde A^i} & S_{G^iG^i} \end{pmatrix} \tag{A33}$$

$$S''_{\text{ghost}} \equiv \begin{pmatrix} 0 & S_{c_ic_i^*} \\ S_{c_i^*c_i} & 0 \end{pmatrix}. \tag{A34}$$

We can then write the tunneling time in Eq. (A14) as

$$\frac{\tau}{T_U} = \frac{R_M^4}{T_U^4}e^{S[\phi_b]}e^{\Delta S_H+\Delta S_t+\Delta S_{gg}}, \tag{A35}$$

where

$$\Delta S_H = \frac{1}{2}\ln\left(\frac{1}{R_M^{10}}\frac{\text{Det}'S''_H[\phi_b]}{\text{Det}S''_H[0]}\right) - \ln J_{\text{trans}} - \ln J_{\text{dil}}, \tag{A36}$$

$$\Delta S_t = -\frac{3}{2}\ln\left(\frac{\text{Det}S''_t[\phi_b]}{\text{Det}S''_t[0]}\right), \tag{A37}$$

$$\Delta S_{gg} = \frac{1}{2}\ln\left(\frac{1}{R_M^6}\frac{\text{Det}'S''_{gg}[\phi_b]}{\text{Det}S''_{gg}[0]}\right) - \frac{1}{2}\ln\left(\frac{\text{Det}S''_{\text{ghost}}[\phi_b]}{\text{Det}S''_{\text{ghost}}[0]}\right) - \ln(16\pi^2 J_{SU(2)}). \tag{A38}$$

Equation (A35) has to be compared with Eq. (14) in the text.

It is important to note that the contribution ΔS_H of Eq. (A36) is greatly modified when the potential with the new physics interactions (A19) replaces the SM potential (A18). Namely, J_{dil} is missing and R^8 rather than R^{10} appears (we have already commented on the size of the bounce to be considered).

Let us compute the different contributions to the fluctuation determinant, (A36), (A37), and (A38), in the two cases of interest for us, namely the case where only SM interactions are considered, the potential given by Eq. (A18) (Sec. II), and the case where we take into account the new physics interactions at the Planck scale, namely the case of the potential (A19) (Sec. III).

Let us begin with the Jacobian factors. As for J_{trans} that appears in Eq. (A36) for ΔS_H, from Eq. (A6) we already know that

$$-\ln J_{\rm trans} = -\ln \frac{S[\phi_b]^2}{4\pi^2}. \tag{A39}$$

In the case of the SM potential alone (Sec. II), Eq. (A18), we have [see Eq. (11)]

$$-\ln J^{\rm SM}_{\rm trans} = -\ln \frac{16\pi^2}{9\lambda^2}. \tag{A40}$$

Inserting the value of λ considered in the text ($\lambda = -0.01345$), we get

$$-\ln J^{\rm SM}_{\rm trans} \sim -11.5. \tag{A41}$$

If we now consider the potential with the inclusion of the new physics interactions (Sec. III), while $\ln J_{\rm trans}$ is still given by Eq. (A39), we no longer have an analytical expression for $S[\phi_b]$. In fact, we compute the bounce solution $\phi_b(x)$ numerically in the next Appendix, so that in turn we obtain $S[\phi_b]$ numerically. For the values of λ, λ_6, and λ_8 considered in the text (see Sec. III), we have

$$-\ln J^{\rm new}_{\rm trans} \sim -5.14. \tag{A42}$$

Let us consider now the contribution of $J_{\rm dil}$ to ΔS_H. As we have already said, the contribution of $J_{\rm dil}$ appears only for the SM case. From Eq. (A12) we see that this contribution is given by

$$\begin{aligned} -\ln J^{\rm SM}_{\rm dil} &= -\frac{1}{2}\ln\left(\frac{1}{2\pi}\int d^4x \left(\frac{\partial\phi_b}{\partial R}\right)^2\right) \\ &= -\frac{1}{2}\ln\left(\frac{8\pi^2}{|\lambda|}\int_0^{\frac{1}{R_M v}} dy y^3 \frac{(y^2-1)^2}{(1+y^2)^4}\right) \\ &= -\frac{1}{2}\ln\left(\frac{8\pi^2}{|\lambda|}\ln\frac{1}{R_M v}\right), \end{aligned} \tag{A43}$$

where we have defined y as $y = r/R_M$. Moreover, the integral over the radial coordinate r is infrared divergent. This is due to the fact that in the potential the mass term has been neglected. For this reason, an infrared cutoff $r = 1/v$ has been inserted, thus getting the above result. By considering the values of λ and R_M given in the text, we get

$$-\ln J^{\rm SM}_{\rm dil} = -6.07. \tag{A44}$$

Finally we move to the contribution of $J_{SU(2)}$ to ΔS_{gg}. From Eq. (A11) we have

$$-\ln(16\pi^2 J_{SU(2)}) = -\frac{3}{2}\ln\left((16\pi^2)^{2/3}\left[\frac{1}{2\pi}\int d^4x \frac{\phi_b^2(r)}{R_M^2}\right]\right). \tag{A45}$$

In the case of the SM potential alone (Sec. II), Eq. (A18), we have

$$\begin{aligned} -\ln(16\pi^2 J_{SU(2)}) &= -\frac{3}{2}\ln\left(\frac{2^{17/3}\pi^{7/3}}{|\lambda|}\int_0^{\frac{1}{R_M v}\gg 1} dy \frac{y^3}{(1+y^2)^2}\right) \\ &= -\frac{3}{2}\ln\left(\frac{2^{17/3}\pi^{7/3}}{|\lambda|}\ln\frac{1}{R_M v}\right), \end{aligned} \tag{A46}$$

where, as for $J_{\rm dil}$, $y = r/R_M$ and we have inserted an infrared cutoff $r = 1/v$. By considering the values of λ and R_M given in the text, we get

$$-\ln(16\pi^2 J^{\rm SM}_{SU(2)}) = -22.6. \tag{A47}$$

If we now consider the potential with the inclusion of the new physics interactions (Sec. III), as for the case of $J_{\rm trans}$, we have to move to the numerical evaluation of the bounce solution (Sec. III and Appendix B). Then, by taking the values of λ, λ_6, and λ_8 considered in the text (see Sec. III), from Eq. (A45) we get

$$-\ln J^{\rm new}_{SU(2)} \sim -15.4. \tag{A48}$$

Let us move now to the computation of the determinants, and focus our attention on ΔS_H, i.e. on S''_H. As is well known, the functional determinant is obtained by solving the eigenvalue equation

$$S''_H \psi = \lambda\psi, \tag{A49}$$

where ψ are the eigenfunctions of S''_H and λ the corresponding eigenvalues. In ΔS_H, the ratio ${\rm Det}' S''_H[\phi_b]/{\rm Det} S''_H[0]$ appears. The prime in the determinant is due to the fact that only the nonzero eigenvalues have to be considered in the evaluation of the determinant.

As $S''_H(\phi_b) = -\partial^2 + V''(\phi_b)$, we have to compute

$$\frac{\det'(-\partial^2 + {\rm V}''(\phi_{\rm b}))}{\det(-\partial^2)}. \tag{A50}$$

Because of radial symmetry, $V''(\phi_b)$ in $[-\partial^2 + V''(\phi_b)]$ depends only on r, and we can use the powerful Gelfand-Yaglom method for the computation of the determinant. Following [48], the logarithm of the ratio of determinants, with some specifications given below, is then obtained as ($j = 0, 1/2, 1, 3/2, 2, \ldots$)

$$\log\left(\frac{\det'(-\partial^2 + {\rm V}''(\phi_{\rm b}))}{\det(-\partial^2)}\right)^{1/2} = \frac{1}{2}\sum_{j=0}^{\infty}(2j+1)^2 \ln\rho_j \tag{A51}$$

$$\text{where } \rho_j = \lim_{r\to\infty}\rho_j(r) \tag{A52}$$

and each of the $\rho_j(r)$ is a solution of the differential equation,

$$\rho_j''(r) + \frac{(4j+3)}{r}\rho_j'(r) - V''(\phi_b(r))\rho_j(r) = 0 \quad \text{(A53)}$$

with boundary conditions $\rho_j(0) = 1$ and $\rho_j'(0) = 0$. [$\rho_j''(r)$ is the second derivative of $\rho_j(r)$ with respect to r….) As for the Laplacian operator ∂^2, we can write it as

$$\partial^2 = \frac{d^2}{dr} + \frac{3}{r}\frac{d}{dr} - \frac{\hat{J}^2}{r^2}, \quad \text{(A54)}$$

where the operator $\hat{J}^2$ is $\hat{J}^2 = \hat{J}_{\mu\nu}\hat{J}_{\mu\nu}$, with $\hat{J}_{\mu\nu} = -\frac{i}{\sqrt{2}}(x_\mu\partial_\nu - x_\nu\partial_\mu)$, "angular momentum operator" in R^4. The eigenfunctions of J^2 are the hyperspherical harmonics $Y_j^{m,m'}$ $(m, m' = -j, \ldots, +j)$ and the eigenvalues are $\lambda_j = 4j(j+1)$, with degeneracy $(2j+1)^2$. Each of the ρ_j is the product of eigenvalues of the operator $S_H''(\phi_b) = -\partial^2 + V''(\phi_b)$ divided by the product of eigenvalues of ∂^2, where the operator $\hat{J}^2$ of Eq. (A54) is replaced by the eigenvalue $4j(j+1)$.

Equation (A51) is ill defined in the following three aspects. One of the eigenvalues related to $j = 0$ is negative, and a second one is vanishing and is related to the dilatation invariance of the theory. Actually, this is true only when we do not consider the presence of new physics interactions, in which case there is no dilatation invariance. Moreover, four of the eigenvalues entering in $\rho_{1/2}$ vanish, as they correspond to the four translational zero modes. Actually ρ_0 and $\rho_{1/2}$ can be separately treated in a standard way [46,48] (see below). Finally, the sum in Eq. (A51) is divergent. This is the usual UV divergence.

If we consider, for instance, the SM case with the $\lambda\phi^4$ potential, inserting the bounce, Eq. (10), in $V''(\phi_b)$ of Eq. (A53), and then taking the limit in Eq. (A52), we have

$$\rho_j = \frac{j(2j-1)}{(j+1)(2j+3)}. \quad \text{(A55)}$$

From the above equation, it is immediate to see that, if we cut the sum in Eq. (A51) to a maximal value of j, say $j = j_{\max}$, we get terms proportional to $j_{\max}$ (quadratic divergences), terms proportional to $\ln j_{\max}$ (logarithmic divergences), finite terms, and then terms $O(1/j_{\max})$.

If we now consider the potential with the insertion of the new physics operators, Eq. (A19), the differential equations (A53) can be solved only numerically. However, also in this case, we can still easily recognize the quadratic and logarithmic divergences as well as the finite contributions.

In order to get rid of these divergences, we have to follow the usual renormalization procedure; i.e. we have to introduce counterterms $\delta S_H^{\rm ct}$, and get for the renormalized sum

$$\left[\frac{1}{2}\sum_{j=0}^{\infty}(2j+1)^2\ln\rho_j\right]_r \equiv \frac{1}{2}\sum_{j=0}^{\infty}(2j+1)^2\ln\rho_j - \delta S_H^{\rm ct}. \quad \text{(A56)}$$

Naturally, the determination of the counterterms depends on the choice of the renormalization conditions and scheme. One possibility consists in extracting the divergences from Eq. (A51) by expanding the ρ_j for large values of j. The first two terms of this expansion provide nothing but the quadratic and logarithmic divergences. By subtracting these terms, we operate a specific choice of counterterms $\delta S_H^{\rm ct}$ that finally would lead to renormalized quantities, in particular to the renormalized quartic coupling.

However, in order to make contact with the existing literature, it is convenient to adopt a more conventional renormalization procedure, namely the $\overline{\rm MS}$ scheme. This amounts to the following procedure [18].

First we solve perturbatively the differential equation for the $\rho_j(r)$, Eq. (A53), by considering $V''(\phi_b)$ as a perturbation, expanding the functions $\rho_j(r)$ as $\rho_j(r) = 1 + \rho_j^{(1)}(r) + \rho_j^{(2)}(r) + \cdots$, and assuming $\rho_j^{(1)}(r) \sim \mathcal{O}(V''(\phi_b))$ and $\rho_j^{(2)}(r) \sim \mathcal{O}(V''(\phi_b)^2)$. Then we take the limit for $r \to \infty$ and compute the expression

$$\sum_{j=0}^{\infty}(2j+1)^2\left(\ln\rho_j - \rho_j^{(1)} + \frac{1}{2}(\rho_j^{(1)})^2 - \rho_j^{(2)}\right), \quad \text{(A57)}$$

which turns out to be finite. This is because the above combination of $\rho^{(1)}$ and $\rho^{(2)}$ has the same divergences of $\ln\rho_j$. Referring again to Eq. (A51), one immediately verifies that such a procedure corresponds to subtract from the first member of Eq. (A51) the first two terms of the perturbative expansion

$$\begin{aligned}&\frac{1}{2}\,\mathrm{Tr}\ln\left[1 + (-\partial^2)^{-1}V''(\phi_b)\right]\\ &= \frac{1}{2}\,\mathrm{Tr}[(-\partial^2)^{-1}V''(\phi_b)]\\ &\quad - \frac{1}{4}\,\mathrm{Tr}[(-\partial^2)^{-1}V''(\phi_b)(-\partial^2)^{-1}V''(\phi_b)] + \mathcal{O}((V'')^3).\end{aligned} \quad \text{(A58)}$$

Finally, the contact with existing literature is made when Eq. (A56) is written by adding and subtracting the quadratic and logarithmic divergencies written once in the form given in Eq. (A57) and once in the form given in Eq. (A58), i.e. by writing

$$\left[\frac{1}{2}\sum_{j=0}^{\infty}(2j+1)^2\ln\rho_j\right]_r$$
$$=\sum_{j=0}^{\infty}(2j+1)^2\left(\ln\rho_j-\rho_j^{(1)}+\frac{1}{2}(\rho_j^{(1)})^2-\rho_j^{(2)}\right)$$
$$+\frac{1}{2}\,\mathrm{Tr}[(-\partial^2)^{-1}V''(\phi_b)]$$
$$-\frac{1}{4}\,\mathrm{Tr}[(-\partial^2)^{-1}V''(\phi_b)(-\partial^2)^{-1}V''(\phi_b)]-\delta S_H^{\mathrm{ct}} \quad \text{(A59)}$$

The sum in the right-hand side of the first line is computed numerically. For the potential in Eq. (A18), i.e. for the potential of the SM alone, the result does not depend on the values of the SM couplings. By performing the numerical computation for this sum, we get 6.02. When we include the couplings λ_6 and λ_8, i.e. when we consider the potential of Eq. (A18), we find that the sum depends on these latter couplings as well as on the other ones. For the numerical example considered in the text, $\lambda_6=-2$ and $\lambda_6=2.1$, and for the central values of the top and Higgs masses, $M_t=173.34$ GeV and $M_H=125.7$ GeV, we finally find for this sum: 2.46.

As for the first two terms in the second line of Eq. (A59), they are nothing but the quadratic and the logarithmic divergences, respectively, and can be computed with the help of ordinary momentum integrals (Fourier space). By computing these integrals within the framework of the $\overline{\mathrm{MS}}$ scheme, and determining the counterterms accordingly, we have

$$\frac{1}{2}\,\mathrm{Tr}[(-\partial^2)^{-1}V''(\phi_b)]$$
$$-\frac{1}{4}\,\mathrm{Tr}[(-\partial^2)^{-1}V''(\phi_b)(-\partial^2)^{-1}V''(\phi_b)]-\delta S_H^{\mathrm{ct},\overline{\mathrm{MS}}}$$
$$=[(1+L)I_1+I_2], \quad \text{(A60)}$$

where $L=\ln(\mu R_M e^{\gamma_E}/2)$, γ_E is the Euler gamma, and

$$I_1=\frac{1}{32}\int\frac{d^4q}{(2\pi)^4}\tilde{V}''(-q)\tilde{V}''(q),$$
$$I_2=\frac{1}{32}\int\frac{d^4q}{(2\pi)^4}\tilde{V}''(-q)\tilde{V}''(q)\ln\left(\frac{2e^{-\gamma_E}}{(q^2)^{1/2}R_M}\right), \quad \text{(A61)}$$

where $\tilde{V}''(q)$ is the Fourier transform of $V''(\phi_b(r))$. For the potential in Eq. (A18), i.e. for the potential of the SM alone, the integrals in Eq. (A61) can be computed analytically and we find $I_1=-3$ and $I_2=1/2$. The renormalized sum of Eq. (A56) is then given by

$$\left[\frac{1}{2}\sum_{j=0}^{\infty}(2j+1)^2\ln\rho_j\right]_r^{\mathrm{SM}}=6.02-\frac{5}{2}-3L. \quad \text{(A62)}$$

Putting together then the results of Eq. (A62), with those of Eqs. (A41), (A44), and (A47), and choosing the renormalization scale (as mentioned above) to make the logarithmic term vanishing ($L=0$), we finally get

$$\Delta S_H^{\mathrm{SM}}=-5.88792. \quad \text{(A63)}$$

For the potential with new physics terms, Eq. (A19), on the contrary, both I_1 and I_2 have to be computed by means of some numerical routine, and the result depends on the value of the couplings. For the value of the parameters given in the text ($\lambda_6=-2$ and $\lambda_8=2.1$), we get $I_1=-6.19$ and $I_2=8.92$. The renormalized sum in Eq. (A56) is now given by

$$\left[\frac{1}{2}\sum_{j=0}^{\infty}(2j+1)^2\ln\rho_j\right]_r^{\mathrm{new}}=2.72856-6.19251\cdot L. \quad \text{(A64)}$$

For the purpose of comparing the two results (with and without the new physics operators), we choose even for this case the same renormalization scale taken above, namely $\mu_{\mathrm{ren}}=2e^{-\gamma_E}/R_M^{\mathrm{SM}}\simeq 2\times 10^{17}$ GeV. The logarithmic term L in this case is not vanishing, as R_M^{new} is different from R_M^{SM}. Putting together then the result of Eq. (A64) with those of Eqs. (A42) and (A48), we finally get ($L=-2.63$)

$$\Delta S_H^{\mathrm{new}}=-9.4425. \quad \text{(A65)}$$

For the evaluation of ΔS_t and ΔS_{gg} in Eqs. (A37) and (A38), we have to follow steps very similar to those used for ΔS_H. The only novelty is that we now have to deal also with (Dirac and/or Lorentz) indices, the eigenfunctions of the corresponding fluctuation operators, $S_t''[\phi_b]$ and $S_{gg}''[\phi_b]$, having an additional algebraic, spinor or vector, structure that can be dealt with in a standard manner [49].

When we consider the SM theory only (SM couplings only), i.e. when the potential of the scalar sector is given by Eq. (A19), the expression for the renormalized determinant appearing in ΔS_t depends only on the ratio of the top Yukawa coupling to the quartic coupling, $g_t^2/|\lambda|$, and turns out to be

$$\left[-\frac{3}{2}\ln\left(\frac{\mathrm{Det}S_t''[\phi_b]}{\mathrm{Det}S_t''[0]}\right)\right]_r^{\mathrm{SM}}=F_t\left(\frac{g_t^2}{|\lambda|}\right)+\frac{g_t^4}{\lambda^2}\left(\frac{5}{6}+L\right)$$
$$+\frac{g_t^2}{|\lambda|}\left(\frac{13}{6}+2L\right), \quad \text{(A66)}$$

where F_t is a numerical function. For the central experimental values of M_H and M_t, where $M_H=125.7$ GeV and $M_t=173.34$ GeV, we find that g_t at the scale $\mu_{\mathrm{ren}}=2e^{-\gamma_E}/R_M\simeq 2\times 10^{17}$ GeV is $g_t=0.40375$ and that $g_t^2/|\lambda|\simeq 12.1184$, and the corresponding F_t is $F_t(g_t^2/|\lambda|)\simeq -193.058$. From Eq. (A66) then, ΔS_t when only SM operators are considered turns out to be

$$\Delta S_t^{\rm SM} \simeq -19.29. \tag{A67}$$

When we consider the potential that involves the contribution of new physics operators, i.e. the potential of Eq. (A19) that contains the contribution of λ_6 and λ_8, ΔS_t has to be computed in a way that is similar to the one used for the Higgs sector, i.e. for ΔS_H. We find

$$\Delta S_t^{\rm new} \simeq -4.98315. \tag{A68}$$

Finally, we have to consider ΔS_{gg}. When the SM interactions only are taken into account, the renormalized determinant appearing in ΔS_{gg} turns out to depend on the two ratios $\frac{g^2}{|\lambda|}$ and $(g^2+g'^2)/|\lambda|$, and we have

$$\begin{aligned}&\left[\frac{1}{2}\ln\left(\frac{1}{R_M^6}\frac{\mathrm{Det}' S''_{gg}[\phi_b]}{\mathrm{Det} S''_{gg}[0]}\right)-\frac{1}{2}\ln\left(\frac{\mathrm{Det} S''_{\rm ghost}[\phi_b]}{\mathrm{Det} S''_{\rm ghost}[0]}\right)\right]_r^{\rm SM}\\ &\quad=\left\{F_g(g^2/|\lambda|)-\left(\frac{6L+5}{9}+\frac{7+6L}{9}\frac{g^2}{|\lambda|}+\frac{1+2L}{16}\frac{g^4}{\lambda^2}\right)\right\}\\ &\qquad+\frac{1}{2}\times\left\{\frac{g^2}{|\lambda|}\to\frac{g^2+g'^2}{|\lambda|}\right\},\end{aligned} \tag{A69}$$

where again F_g is a numerical function. We find that the renormalized couplings at the renormalization scale $\mu_{\rm ren} = 2e^{-\gamma_E}/R_M \simeq 2\times 10^{17}$ GeV are $g = 0.5168$ and $g' = 0.459068$, which in turn gives $g^2/|\lambda| \simeq 19.8562$ and $(g^2+g'^2)/|\lambda| \simeq 35.5228$. Moreover, $F_g(g^2/|\lambda|) \simeq 93.9308$ and $F_g((g^2+g'^2)/|\lambda|) \simeq 380.344$. Therefore, putting together these results with those of Eq. (A47) we find

$$\Delta S_{gg}^{\rm SM} \simeq 67.4064. \tag{A70}$$

Once again, when we consider the potential (A19) with the contribution of new physics interactions, and therefore the contribution of the additional couplings λ_6 and λ_8, the expression corresponding to Eq. (A69) can be computed only numerically. Performing this computation, and then including the contribution of Eq. (A48), we finally find

$$\Delta S_{gg}^{\rm new} \simeq 8.42902. \tag{A71}$$

This latter result completes the work of this Appendix. Actually, by collecting all of the quantum fluctuation contributions ΔS_i, discussed in the present Appendix, the tables for the loop contribution to τ presented in Secs. II and III are obtained.

APPENDIX B NUMERICAL BOUNCE SOLUTIONS

In this Appendix we present the numerical determination of the bounce solution to Eq. (25) of Sec. III in the text, with boundary conditions given by Eqs. (26) and (27). These boundary conditions at $x = 0$ and $x = \infty$ are implemented by first considering a minimal and a maximal value of x, $x_{\rm min}$, and $x_{\rm max}$, and then studying the convergence of the solution (to the desired level of accuracy) by taking lower and lower values of $x_{\rm min}$ and higher and higher values of $x_{\rm max}$. As described in Ref. [5], one technique is to guess values of $\phi(0)$ and integrate outward. If the value of $\phi(0)$ is too large, then ϕ will overshoot the value of ϕ at the false vacuum, whereas if it is too small, it will undershoot. So one can gradually converge on the correct value. However, the forward-backward shooting method converges more quickly.

To proceed with such an analysis, however, we first need to study analytically the asymptotical behavior of Eq. (25) around $x = 0$ and $x = \infty$. Let us begin by performing an expansion of $\varphi(x)$ in powers of x around $x = 0$. For our purposes, it is sufficient to consider an expansion up to x^8. We write only the first few terms,

$$\varphi(x) = B_0 + B_2 x^2 + B_3 x^3 + \cdots, \tag{B1}$$

where, due to the condition $\varphi'(0) = 0$, the linear term is missing. Inserting the expansion (B1) in (25), we find that the coefficients of odd powers of x vanish, while those of even powers of x are all given in terms of B_0 (from now on indicated with B),

$$\varphi(x) = B + (\lambda B^3 + \lambda_6 B^5 + \lambda_8 B^7)\frac{x^2}{8} + \cdots, \tag{B2}$$

where only the first and the second terms of the expansion are explicitly written.

As we shall see in a moment, the coefficient of x^2 (for the case of interest to us) is negative and Eq. (B2) shows that, for values of x close to $x = 0$, the bounce behaves as an upside down parabola. This observation is very useful for our numerical analysis.

Let us study now the asymptotic region $x \to \infty$. As the bounce has to fulfill the condition (26), we expand $\varphi(x)$ in powers of $1/x$. For our purposes, we perform the expansion up to $1/x^{20}$. Writing again only the first few terms,

$$\varphi(x) = \frac{A_1}{x} + \frac{A_2}{x^2} + \frac{A_3}{x^3} + \frac{A_4}{x^4} + \cdots. \tag{B3}$$

Inserting the expansion (B3) in (25), we find that the coefficients of odd powers of $1/x$ vanish, while those of even powers are all written in terms of A_2 (from now on indicated with A)

$$\varphi(x) = \frac{A}{x^2} - \frac{\lambda}{8}\frac{A^3}{x^4} + \cdots, \tag{B4}$$

where, as for Eq. (B2), only the first and the second terms are explicitly written. Equation (B4) shows that, for large values of x, $\varphi(x)$ behaves as $1/x^2$. As we shall see in a

moment, this observation is very useful for our numerical analysis.

Let us proceed now with the forward-backward shooting. Going back to Eq. (B2), we choose a value of x close to $x = 0$, say $x = x_{\min} \ll 1$, and consider the two "initial conditions" $\varphi(x_{\min})$ and $\varphi'(x_{\min})$,

$$\varphi(x_{\min}) = B + (\lambda B^3 + \lambda_6 B^5 + \lambda_8 B^7)\frac{x_{\min}^2}{8} + \cdots,$$
$$\varphi'(x_{\min}) = (\lambda B^3 + \lambda_6 B^5 + \lambda_8 B^7)\frac{x_{\min}}{4} + \cdots \quad \text{(B5)}$$

for the integration of the second order differential equation (25). Choosing also a value $x = x_{\max} \gg 1$, Eq. (25) is integrated, for different choices of B, in the range $[x_{\min}, x_{\max}]$.

As from (B4) we know that, for large values of x, $\varphi(x)$ behaves as $1/x^2$, the search for the bounce is realized by *tuning* B so that, for large values of x (actually up to $x_{\max}$), the product $x^2\varphi(x)$ reaches a plateau. This completes the "forward" part of the method. For the "backward" part, we have to follow similar steps, but starting from large values of x and integrating back our differential equation (25) toward small values.

Let us study now this equation for the values of the coupling constants considered in the text, namely $\lambda = -0.01345$, $\lambda_6 = -2$, and $\lambda_8 = 2.1$. The forward shooting described above is illustrated in Fig. 8, where $x^2\varphi(x)$ is plotted against x. For the integration range, we have chosen $x_{\min} = 6 \times 10^{-2}$ and $x_{\max} = 10^2$.

The central part of the forward shooting is the tuning of the parameter B. In Fig. 8, we plot three curves $x^2\varphi(x)$ for

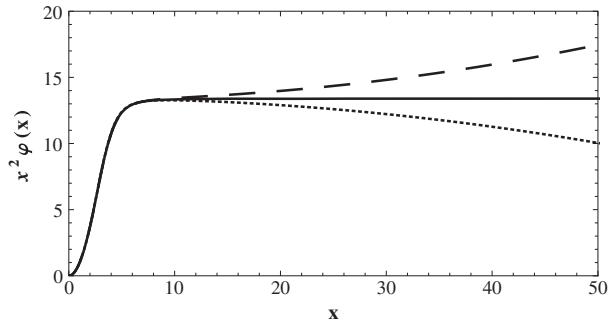

FIG. 8. Plot of $x^2\varphi(x)$, for three different solutions of Eq. (25), with $\lambda = -0.01345$, $\lambda_6 = -2$, and $\lambda_8 = 2.1$. The x range goes from $x = x_{\min} = 6 \times 10^{-2}$ to $x = 50$, although the numerical integration is performed up to $x_{\max} = 10^2$. This figure well illustrates the forward shooting. Equation (25) is integrated starting with the initial values (B5) for $\varphi(x_{\min})$ and $\varphi'(x_{\min})$ at $x = x_{\min} = 6 \times 10^{-2}$. The parameter B is tuned until $x^2\varphi(x)$ saturates to a plateau for values of x greater than $x_{\min}$ and at least up to $x_{\max}$. We see that for $B = 0.967$ (dotted line) and $B = 0.9665$ (dashed line), $x^2\varphi(x)$ diverges downwards and upwards, respectively. For $B = 0.966777$ (solid line), the plateau is reached and our first approximation to the bounce is obtained.

three different values of B. Although the x range in the figure goes from $x = x_{\min} = 6 \times 10^{-2}$ to $x = 50$, the numerical integration is performed from $x_{\min} = 6 \times 10^{-2}$ up to $x_{\max} = 10^2$. The dotted line is obtained for $B = 0.967$. After a first transient regime, from $x = x_{\min}$ up to $x \sim 5$, the product $x^2\varphi(x)$ becomes almost constant in the range from $x \sim 5$ to $x \sim 10$. For $x > 10$, however, it starts to decrease, so that the corresponding $\varphi(x)$ does not satisfy the asymptotic condition $\varphi(x) \propto 1/x^2$.

For a lower value of B, $B = 0.9665$, the product $x^2\varphi(x)$ is given by the dashed line of Fig. 8. Again, after a first transient regime, $x^2\varphi(x)$ becomes almost constant in the range from $x \sim 5$ to $x \sim 10$. For $x > 10$, however, $x^2\varphi(x)$ starts to increase, again violating the asymptotic condition $\varphi(x) \propto 1/x^2$. Finally, continuing with the tuning of B, it is found that, for $B = 0.966777$ (solid line), the product $x^2\varphi(x)$ turns out to reach a plateau up to $x = x_{\max}$ (in the figure the x range is extended only up to $x = 50$). The corresponding numerical solution $\varphi(x)$ is then our first estimate of the bounce (in the range $x_{\min} \le x \le x_{\max}$).

The next step of our numerical procedure is the backward shooting, where we integrate backward Eq. (25) from the upper limit $x_{\max}$ of the previous (forward) integration, $x_{\max} = 10^2$, and extend the integration domain down to $x'_{\min} = 10^{-2} < x_{\min}$. The initial conditions are taken from the asymptotic behavior of the bounce, Eq. (B4),

$$\varphi(x_{\max}) = \frac{A}{x_{\max}^2} - \frac{\lambda}{8}\frac{A^3}{x_{\max}^4} + \cdots,$$
$$\varphi'(x_{\max}) = -\frac{2A}{x_{\max}^3} + \frac{\lambda}{2}\frac{A^3}{x_{\max}^5} + \cdots. \quad \text{(B6)}$$

Similar to the forward case, we have to fine-tune the parameter A so that, according to (B2), the solution $\varphi(x)$, for small values of x, satisfies the condition

$$\frac{\varphi'(x)}{x} \simeq \text{const} \quad \text{(B7)}$$

in the range $[x'_{\min}, x_{\max}]$.

In Fig. 9 we plot $\varphi'(x)/x$ versus x for three different values of A and illustrate how the fine-tuning of A is realized. The domain of our numerical (backward) integration ranges from $x_{\max} = 10^2$ down to $x'_{\min} = 10^{-2}$, although in the figure we only show the range from $x'_{\min} = 10^{-2}$ to $x = 0.15$.

The dotted line is obtained for $A = 13.37292731$. As we approach smaller and smaller values of x, $\varphi'(x)/x$ starts to decrease, thus violating the bounce condition $\varphi'(x)/x \sim \text{const}$. The dashed line is obtained for $A = 13.37292732$. For smaller and smaller values of x, $\varphi'(x)/x$ starts to increase, again violating the bounce condition. Finally, for $A = 13.372927315215$, the ratio $\varphi'(x)/x$ reaches a plateau, thus showing that this is the

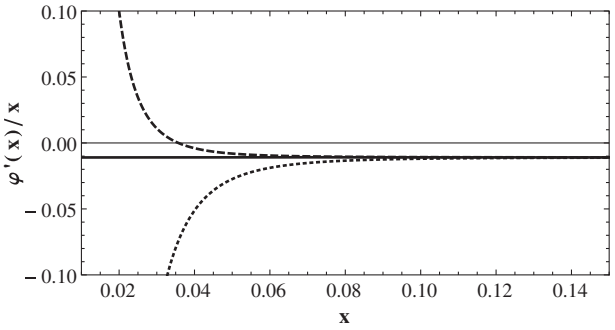

FIG. 9. The backward shooting with a plot of $\varphi'(x)/x$ for three different solutions of Eq. (25) ($\lambda = -0.01345$, $\lambda_6 = -2$, $\lambda_8 = 2.1$). The x range goes from $x_{\min} = 10^{-2}$ to $x = 0.15$, although the numerical integration is performed from $x_{\max} = 10^2$ down to $x_{\min} = 10^{-2}$. Equation (25) is integrated with initial values (B6) for $\varphi(x_{\max})$ and $\varphi'(x_{\max})$. The parameter A is tuned until $\varphi'(x)/x$ saturates to a plateau for small values of x. For $A = 13.37292731$ (dotted line) and $A = 13.37292732$ (dashed line), $\varphi'(x)/x$ diverges downwards and upwards, respectively. Finally, for $A = 13.372927315215$ (solid line), the plateau is reached. We have then, to a very high degree of numerical accuracy, the bounce solution to our equation.

value of A that corresponds to the bounce solution (at this order of numerical precision).

We can then iterate the procedure of forward and backward integrations by enlarging the range of integration, thus obtaining values of A and B with a higher and higher degree of numerical accuracy.

APPENDIX C SU(5) AND LOW ENERGY THEORY

Here we consider a toy grand unified model which gives Eq. (22) as the effective low energy theory. Note that nothing we have done in this paper involves gravity, and thus M_P can be replaced by the unification scale, M_X. Note that if $M_X \ll M_P$, the effective values of λ_6 and λ_8 would be much larger, leading to even bigger effects, and thus the conservative approach is to consider the case in which $M_X \sim M_P$.

We will consider the minimal $SU(5)$ model broken at the M_P scale. Such a model, of course, is phenomenologically unacceptable, but if this model gives the potential of Eq. (22) with $O(1)$ coefficients, then clearly a more complicated (and acceptable) grand unified theory can also do so. The symmetry is broken down to $SU(3) \times SU(2) \times U(1)$ with the minimal Higgs content of a 24-plet, and the breaking of the Standard Model group uses a 5-plet.

The Higgs potential is given, with Ψ being the 24 and ϕ being the 5, by

$$V(\Psi) = -\frac{1}{2}\mu^2 \mathrm{Tr}(\Psi^2) + \frac{1}{4}a(\mathrm{Tr}(\Psi^2))^2 + \frac{1}{2}b\mathrm{Tr}(\Psi^4), \tag{C1}$$

$$V(\phi) = -\frac{1}{2}\nu^2\phi^\dagger\phi + \frac{1}{4}\lambda(\phi^\dagger\phi)^2, \tag{C2}$$

$$V(\Phi,\phi) = \alpha\phi^\dagger\phi\mathrm{Tr}(\Psi^2) + \beta\phi^\dagger\Psi^2\phi. \tag{C3}$$

The relevant Higgs fields in the 24 are the Ψ_3 and the Ψ_0, where Ψ_3 is the neutral member of the color-singlet, isotriplet and Ψ_0 is the isosinglet.

The diagrams leading to higher order operators in the effective low-energy theory (below M_P) to leading order in the couplings are shown in Fig. 10. For the ϕ^6 term, there are two diagrams, one with three Ψ_0 fields and one with two Ψ_3 fields and one Ψ_0 field. Using the vertices found in Ref. [50], we find that the contributions to λ_6 are

$$5\frac{(\frac{1}{4}\alpha + \frac{3}{40}\beta)^3}{(15a+7b)^2} \tag{C4}$$

for the first, and

$$\frac{1}{10}\left(\frac{3}{4}\right)^4 \frac{5a+9b}{15a+7b}\left(\frac{1}{10}\alpha + \frac{3}{100}\beta\right)\frac{\beta^2}{b^2} \tag{C5}$$

for the second. We have chosen the scale M_P to equal the vacuum expectation value (vev) of the 24-plet (which is numerically very close to the gauge boson mass).

Now, in order to have the correct symmetry breaking pattern, β must be negative, and $15a + 7b$ and b must be positive. But $\alpha + \frac{3}{10}\beta$ can have either sign. So if α, for example, equals ± 4 (well below the unitarity bound, see [50]), β is small, and $15a + 7b$ is, say, 1, then the contribution to λ_6 is ± 2, showing that a large coefficient is not unreasonable, and is well within unitarity limits. Of course, the contribution to λ_6 would be even larger if, as expected, the unification scale is well below the Planck scale.

For the ϕ^8 term, one has three diagrams, one with four Ψ_0, one with four Ψ_3, and one with two of each (there are six copies from combinatorics). The contributions to λ_8 are

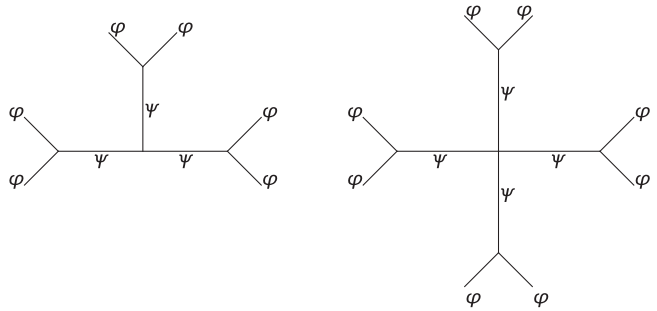

FIG. 10. Diagrams leading to higher dimensional operators in the low energy theory. ϕ is the Standard Model Higgs and Ψ is the 24-plet.

$$\frac{8}{7}\frac{(\frac{1}{4}\alpha+\frac{3}{40}\beta)^4}{(15a+7b)^3} \tag{C6}$$

from the first. This term numerically dominates for most of the parameter space. The second gives

$$\frac{(\frac{3}{40}\beta)^4}{(2b)^4}, \tag{C7}$$

and the third gives

$$\left(\frac{3}{20}\right)^4\frac{(5a+9b)(\frac{1}{4}\alpha+\frac{3}{40}\beta)^2}{(10b)^2(15a+7b)^2}. \tag{C8}$$

Again, these can easily be large and still be within unitarity bounds, even if the unification scale is at the Planck scale. Note that the expressions are positive, and thus Eq. (22) would be bounded. Also note that, to leading order, there are no ϕ^{10} terms, further justifying the truncation in Eq. (22).

This model is not to be taken too seriously, of course, but does demonstrate how a very simple unified theory can give the effective low energy theory of Eq. (22).

[1] N. Cabibbo, L. Maiani, G. Parisi, and R. Petronzio, Nucl. Phys. **B158**, 295 (1979).
[2] R. A. Flores and M. Sher, Phys. Rev. D **27**, 1679 (1983).
[3] M. Lindner, Z. Phys. C **31**, 295 (1986).
[4] D. L. Bennett, H. B. Nielsen, and I. Picek, Phys. Lett. B **208**, 275 (1988).
[5] M. Sher, Phys. Rep. **179**, 273 (1989).
[6] M. Lindner, M. Sher, and H. W. Zaglauer, Phys. Lett. B **228**, 139 (1989).
[7] P. B. Arnold, Phys. Rev. D **40**, 613 (1989).
[8] G. Anderson, Phys. Lett. B **243**, 265 (1990).
[9] P. Arnold and S. Vokos, Phys. Rev. D **44**, 3620 (1991).
[10] C. Ford, D. R. T. Jones, P. W. Stephenson, and M. B. Einhorn, Nucl. Phys. **B395**, 17 (1993).
[11] M. Sher, Phys. Lett. B **317**, 159 (1993).
[12] G. Altarelli and G. Isidori, Phys. Lett. B **337**, 141 (1994).
[13] J. A. Casas, J. R. Espinosa, and M. Quirós, Phys. Lett. B **342**, 171 (1995).
[14] J. R. Espinosa and M. Quirós, Phys. Lett. B **353**, 257 (1995).
[15] J. A. Casas, J. R. Espinosa, and M. Quirós, Phys. Lett. B **382**, 374 (1996).
[16] C. D. Froggatt and H. B. Nielsen, Phys. Lett. B **368**, 96 (1996).
[17] C. D. Froggatt, H. B. Nielsen, and Y. Takanishi, Phys. Rev. D **64**, 113014 (2001).
[18] G. Isidori, G. Ridolfi, and A. Strumia, Nucl. Phys. **B609**, 387 (2001).
[19] J. R. Espinosa, G. F. Giudice, and A. Riotto, J. Cosmol. Astropart. Phys. 05 (2008) 002.
[20] J. Ellis, J. R. Espinosa, G. F. Giudice, A. Hoecker, and A. Riotto, Phys. Lett. B **679**, 369 (2009).
[21] J. Elias-Miro, J. R. Espinosa, G. F. Giudice, G. Isidori, A. Riotto, and A. Strumia, Phys. Lett. B **709**, 222 (2012).
[22] G. Degrassi, S. Di Vita, J. Elias-Miro, J. R. Espinosa, G. F. Giudice, G. Isidori, and A. Strumia, J. High Energy Phys. 08 (2012) 098.
[23] D. Buttazzo, G. Degrassi, P. P. Giardino, G. F. Giudice, F. Sala, A. Salvio, and A. Strumia, J. High Energy Phys. 12 (2013) 089.
[24] ATLAS Collaboration, Phys. Lett. B **710**, 49 (2012).
[25] CMS Collaboration, Phys. Lett. B **710**, 26 (2012).
[26] S. Alekhin, A. Djouadi, and S. Moch, Phys. Lett. B **716**, 214 (2012).
[27] G. Degrassi, Nuovo Cimento Soc. Ital. Fis. C **037**, 47 (2014).
[28] F. L. Bezrukov and M. Shaposhnikov, Phys. Lett. B **659**, 703 (2008); J. High Energy Phys. 07 (2009) 089; F. L. Bezrukov, A. Magnin, and M. Shaposhnikov, Phys. Lett. B **675**, 88 (2009).
[29] Y. Hamada, K. y. Oda, and F. Takahashi, Phys. Rev. D **90**, 097301 (2014).
[30] Y. Hamada, H. Kawai, K. y. Oda, and S. C. Park, arXiv:1408.4864
[31] K. Bhattacharya, J. Chakrabortty, S. Das, and T. Mondal, J. Cosmol. Astropart. Phys. 12 (2014) 001
[32] A. Datta, B. L. Young, and X. Zhang, Phys. Lett. B **385**, 225 (1996)
[33] A. Kobakhidze and A. Spencer-Smith, Phys. Lett. B **722**, 130 (2013)
[34] M. Torabian, arXiv:1410.1744
[35] N. Khan and S. Rakshit, Phys. Rev. D **90**, 113008 (2014).
[36] S. Coleman, Phys. Rev. D **15**, 2929 (1977).
[37] P. H. Frampton, Phys. Rev. Lett. **37**, 1378 (1976); **37**, 1716 (E) (1976).
[38] C. G. Callan and S. Coleman, Phys. Rev. D **16**, 1762 (1977).
[39] V. Branchina and E. Messina, Phys. Rev. Lett. **111**, 241801 (2013).
[40] V. Branchina, arXiv:1405.7864.
[41] V. Branchina, E. Messina, and A. Platania, J. High Energy Phys. 09 (2014) 182.
[42] A. Kusenko, K. M. Lee, and E. J. Weinberg, Phys. Rev. D **55**, 4903 (1997).
[43] L. N. Mihaila, J. Salomon, and M. Steinhauser, Phys. Rev. Lett. **108**, 151602 (2012).

[44] K. Chetyrkin and M. Zoller, J. High Energy Phys. 06 (2012) 033.
[45] F. Bezrukov, M. Yu. Kalmykov, B. A. Kniehl, and M. Shaposhnikov, J. High Energy Phys. 10 (2012) 140.
[46] G. V. Dunne and H. Min, Phys. Rev. D **72**, 125004 (2005).
[47] K. Lee and E. J. Weinberg, Nucl. Phys. **B267**, 181 (1986).
[48] G. Dunne, J. Phys. A **41**, 304006 (2008).
[49] A. Pais, Proc. Natl. Acad. Sci. U.S.A. **40**, 835 (1954); M. Daumens and P. Minnaert, J. Math. Phys. (N.Y.) **17**, 1903 (1976).
[50] H. Huffel, Z. Phys. C **10**, 327 (1981).